

We are IntechOpen, the world's leading publisher of Open Access books Built by scientists, for scientists

6,900

Open access books available

186,000

International authors and editors

200M

Downloads

Our authors are among the

154

Countries delivered to

TOP 1%

most cited scientists

12.2%

Contributors from top 500 universities



WEB OF SCIENCE™

Selection of our books indexed in the Book Citation Index
in Web of Science™ Core Collection (BKCI)

Interested in publishing with us?
Contact book.department@intechopen.com

Numbers displayed above are based on latest data collected.
For more information visit www.intechopen.com



A Frequency Domain Quantitative Technique for Robust Control System Design

José Luis Guzmán¹, José Carlos Moreno², Manuel Berenguel³, Francisco Rodríguez⁴, Julián Sánchez-Hermosilla⁵

^{1,2,3,4}Departamento de Lenguajes y Computación;

⁵Departamento de Ingeniería Rural, University of Almería
Spain

1. Introduction

Most control techniques require the use of a plant model during the design phase in order to tune the controller parameters. The mathematical models are an approximation of real systems and contain imperfections by several reasons: use of low-order descriptions, unmodelled dynamics, obtaining linear models for a specific operating point (working with poor performance outside of this working point), etc. Therefore, control techniques that work without taking into account these modelling errors, use a fixed-structure model and known parameters (nominal model) supposing that the model exactly represents the real process, and the imperfections will be removed by means of feedback. However, there exist other control methods called robust control techniques which use these imperfections implicitly during the design phase. In the robust control field such imperfections are called uncertainties, and instead of working only with one model (nominal model), a family of models is used forming the *nominal model + uncertainties*. The uncertainties can be classified in parametric or structured and non-parametric or non-structured. The first ones allow representing the uncertainties into the model coefficients (e.g. the value of a pole placed between maximum and minimum limits). The second ones represent uncertainties as unmodelled dynamics (e.g. differences in the orders of the model and the real system) (Morari and Zafiriou, 1989).

The robust control technique which considers more exactly the uncertainties is the Quantitative Feedback Theory (QFT). It is a methodology to design robust controllers based on frequency domain, and was developed by Prof. Isaac Horowitz (Horowitz, 1982; Horowitz and Sidi, 1972; Horowitz, 1993). This technique allows designing robust controllers which fulfil some minimum quantitative specifications considering the presence of uncertainty in the plant model and the existence of perturbations. With this theory, Horowitz showed that the final aim of any control design must be to obtain an open-loop transfer function with the suitable bandwidth (cost of feedback) in order to sensitize the plant and reduce the perturbations. The Nichols plane is used to achieve a desired robust design over the specified region of plant uncertainty where the aim is to design a compensator $C(s)$ and a prefilter $F(s)$ (if it is necessary) (see Figure 1), so that performance and stability specifications are achieved for the family of plants.

This chapter presents for SISO (Single Input Single Output) LTI (Linear Time Invariant) systems, a detailed description of this robust control technique and two real experiences where QFT has successfully applied at the University of Almería (Spain). It starts with a QFT description from a theoretical point of view, afterwards section 3.1 is devoted to present two well-known software tools for QFT design, and after that two real applications in agricultural spraying tasks and solar energy are presented. Finally, the chapter ends with some conclusions.

2. Synthesis of SISO LTI uncertain feedback control systems using QFT

QFT is a methodology to design robust controllers based on frequency domain (Horowitz, 1993; Yaniv, 1999). This technique allows designing robust controllers which fulfil some quantitative specifications. The Nichols plane is the key tool for this technique and is used to achieve a robust design over the specified region of plant uncertainty. The aim is to design a compensator $C(s)$ and a prefilter $F(s)$ (if it is necessary), as shown in Figure 1, so that performance and stability specifications are achieved for the family of plants $\varphi(s)$ describing a plant $P(s)$. Here, the notation \hat{a} is used to represent the Laplace transform for a time domain signal $a(t)$.

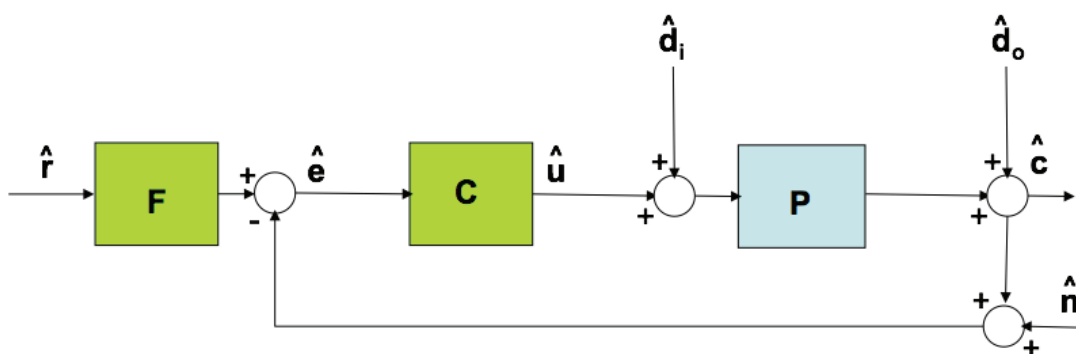


Fig. 1. Two degrees of freedom feedback system.

The QFT technique uses the information of the plant uncertainty in a quantitative way, imposing robust tracking, robust stability, and robust attenuation specifications (among others). The 2DoF compensator $\{F, C\}$, from now onwards the s argument will be omitted when necessary for clarity, must be designed in such a way that the plant behaviour variations due to the uncertainties are inside of some specific tolerance margins in closed-loop. Here, the family $\varphi(s)$ is represented by the following equation

$$\varphi(s) = \left\{ P(s) = k \frac{\prod_{i=1}^n (s + z_i) \prod_{z=1}^m (s^2 + 2\zeta_z \omega_{0z} s + \omega_{0z}^2)}{s^N \prod_{r=1}^a (s + p_r) \prod_{t=1}^b (s^2 + 2\zeta_t \omega_{0t} s + \omega_{0t}^2)} : \right. \quad (1)$$

$$\left. \begin{aligned} k &\in [k_{min}, k_{max}], z_i \in [z_{i,min}, z_{i,max}], p_r \in [p_{r,min}, p_{r,max}], \\ \zeta_z &\in [\zeta_{z,min}, \zeta_{z,max}], \omega_{0z} \in [\omega_{0z,min}, \omega_{0z,max}], \\ \zeta_t &\in [\zeta_{t,min}, \zeta_{t,max}], \omega_{0t} \in [\omega_{0t,min}, \omega_{0t,max}], \\ &n + m < a + b + N \end{aligned} \right\}$$

A typical QFT design involves the following steps:

1. *Problem specification.* The plant model with uncertainty is identified, and a set of working frequencies is selected based on the system bandwidth, $\Omega = \{\omega_1, \omega_2, \dots, \omega_k\}$. The specifications (stability, tracking, input disturbances, output disturbances, noise, and control effort) for each frequency are defined, and the nominal plant P_0 is selected.
2. *Templates.* The quantitative information of the uncertainties is represented by a set of points on the Nichols plane. This set of points is called *template* and it defines a graphical representation of the uncertainty at each design frequency ω . An example is shown in Figure 2, where templates of a second-order system given by $P(s) = k/s(s+a)$, with $k \in [1, 10]$ and $a \in [1, 10]$ are displayed for the following set of frequencies $\Omega = \{0.5, 1, 2, 4, 8, 15, 30, 60, 90, 120, 180\}$ rad/s.
3. *Bounds.* The specifications settled at the first step are translated, for each frequency ω in Ω set, into prohibited zones on the Nichols plane for the loop transfer function $L_0(j\omega) = C(j\omega)P_0(j\omega)$. These zones are defined by limits that are known as *bounds*. There exist so many *bounds* for each frequency as specifications are considered. So, all these *bounds* for each frequency are grouped showing an unique prohibited *boundary*. Figure 3 shows an example for stability and tracking specifications.

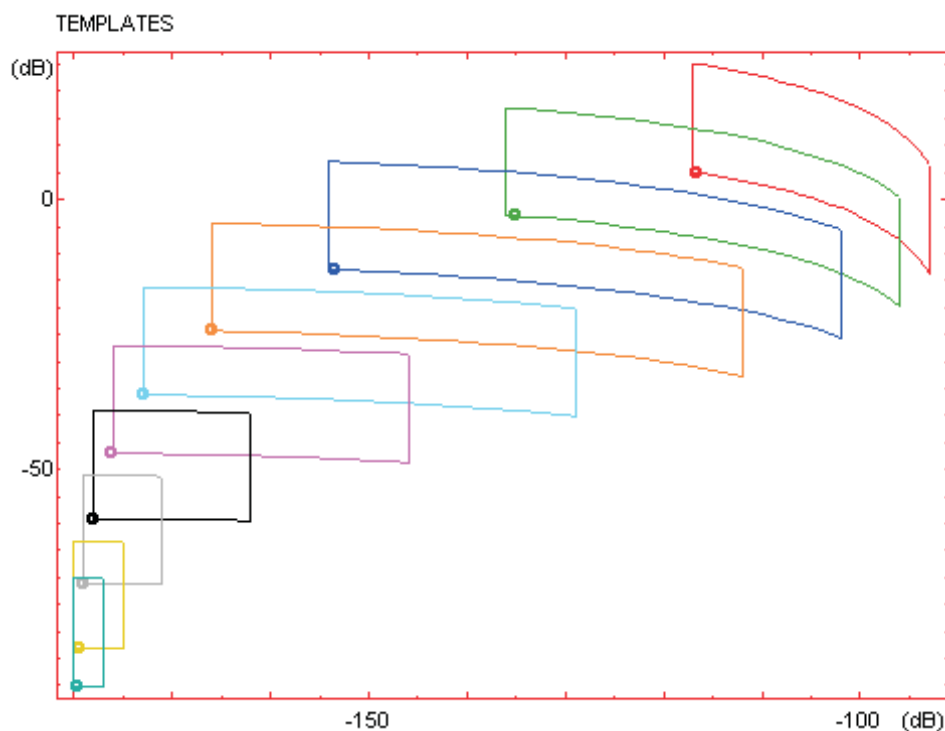


Fig. 2. QFT Template example.

4. *Loop shaping.* This phase consists in designing the C controller in such a way that the nominal loop transfer function $L_0(j\omega) = C(j\omega)P_0(j\omega)$ fulfils the *bounds* calculated in the previous phase. Figure 3 shows the design of L_0 where the *bounds* are fulfilled at each design frequency.
5. *Prefilter.* The prefilter F is designed so that the closed-loop transfer function from reference to output follows the robust tracking specifications, that is, the closed-loop system variations must be inside of a desired tolerance range, as Figure 4 shows.

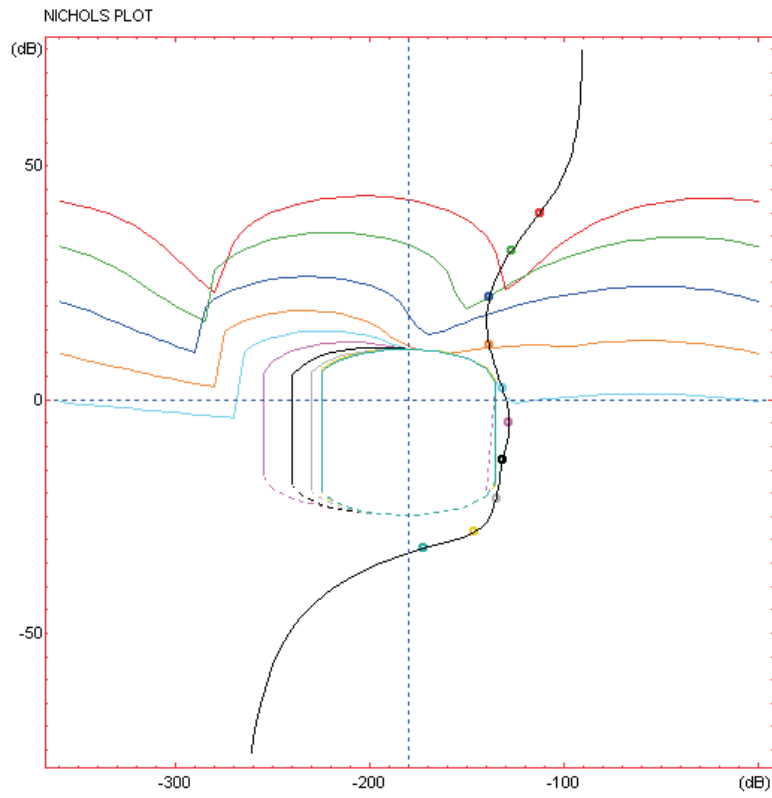


Fig. 3. QFT Bound and Loop Shaping example.

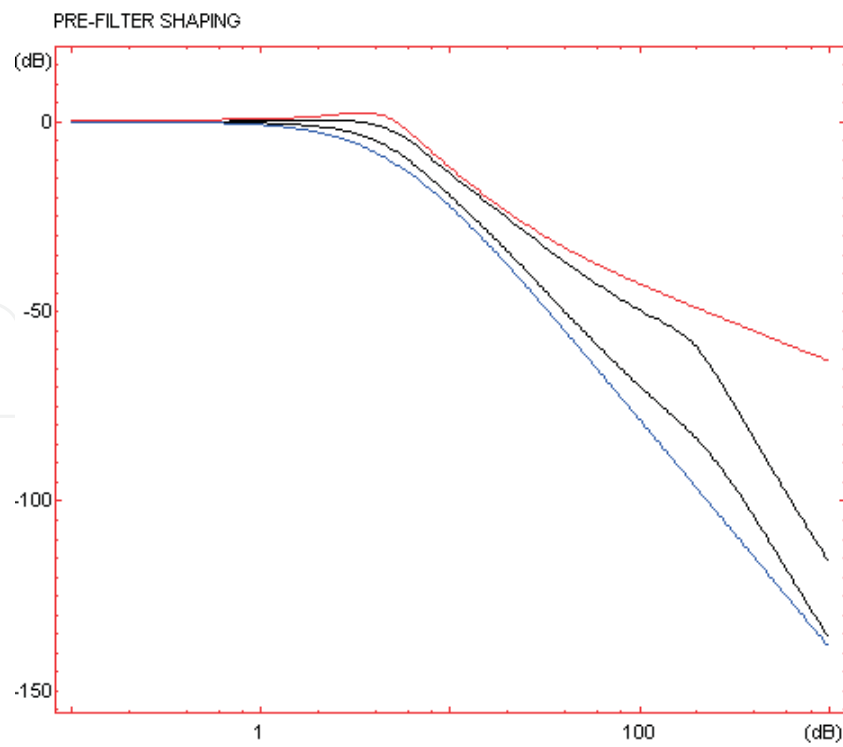


Fig. 4. QFT Prefilter example.

6. *Validation*. This step is devoted to verify that the closed-loop control system fulfils, for the whole family of plants, and for all frequencies in the bandwidth of the system, all the specifications given in the first step. Otherwise, new frequencies are added to the set Ω , so that the design is repeated until such specifications are reached.

The closed-loop specifications for system in Figure 1 are typically defined in time domain and/or in the frequency domain. The time domain specifications define the desired outputs for determined inputs, and the frequency domain specifications define in terms of frequency the desired characteristics for the system output for those inputs.

In the following, these types of specifications are described and the specifications translation problem from time domain to frequency domain is considered.

2.1 Time domain specifications

Typically, the closed-loop specifications for system in Figure 1 are defined in terms of the system inputs and outputs. Both of them must be delimited, so that the system operates in a predetermined region. For example:

1. In a regulation problem, the aim is to achieve a plant output close to zero (or nearby a determined operation point). For this case, the time domain specifications could define allowed operation regions as shown in Figures 5a and 5b, supposing that the aim is to achieve a plant output close to zero.
2. In a reference tracking problem, the plant output must follow the reference input with determined time domain characteristics. In Figure 5c a typical specified region is shown, in which the system output must stay. The unit step response is a very common characterization, due to it combines a fast signal (an infinite change in velocity at $t = 0^+$) with a slow signal (it remains in a constant value after transitory).

The classical specifications such as rise time, settling time and maximum overshoot, are special cases of examples in Figure 5. All these cases can be also defined in frequency domain.

2.2 Frequency domain specifications

The closed-loop specifications for system in Figure 1 are typically defined in terms of inequalities on the closed-loop transfer functions for the system, as shown in Equations (2)-(7).

1. Disturbance rejection at the plant output:

$$\left| \frac{\hat{c}}{\hat{d}_o} \right| = \left| \frac{1}{1 + P(j\omega)C(j\omega)} \right| \leq \delta_{po}(\omega) \quad \forall \omega > 0, \forall P \in \wp \quad (2)$$

2. Disturbance rejection at the plant input:

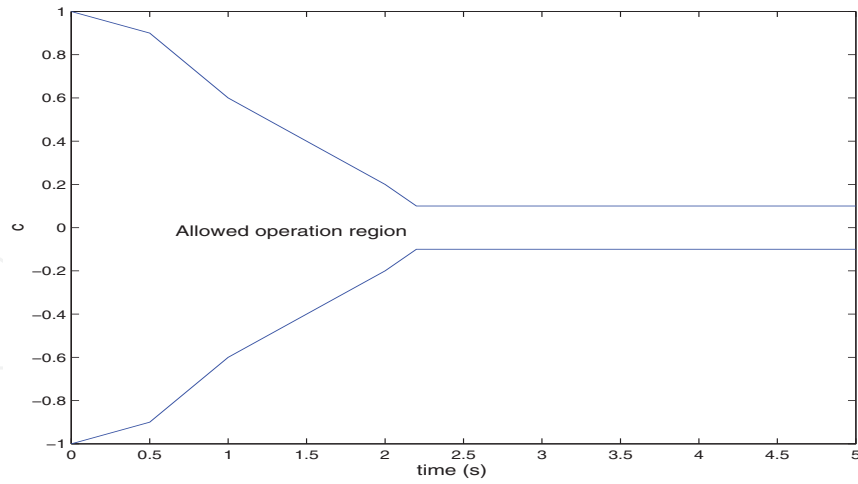
$$\left| \frac{\hat{c}}{\hat{d}_i} \right| = \left| \frac{P(j\omega)}{1 + P(j\omega)C(j\omega)} \right| \leq \delta_{pi}(\omega) \quad \forall \omega > 0, \forall P \in \wp \quad (3)$$

3. Stability:

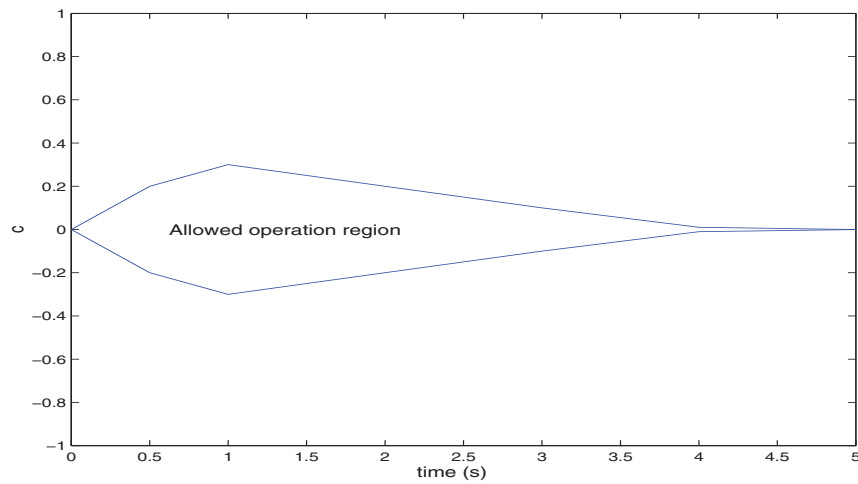
$$\left| \frac{\hat{c}}{\hat{r}F} \right| = \left| \frac{P(j\omega)C(j\omega)}{1 + P(j\omega)C(j\omega)} \right| \leq \lambda \quad \forall \omega > 0, \forall P \in \wp \quad (4)$$

4. References Tracking:

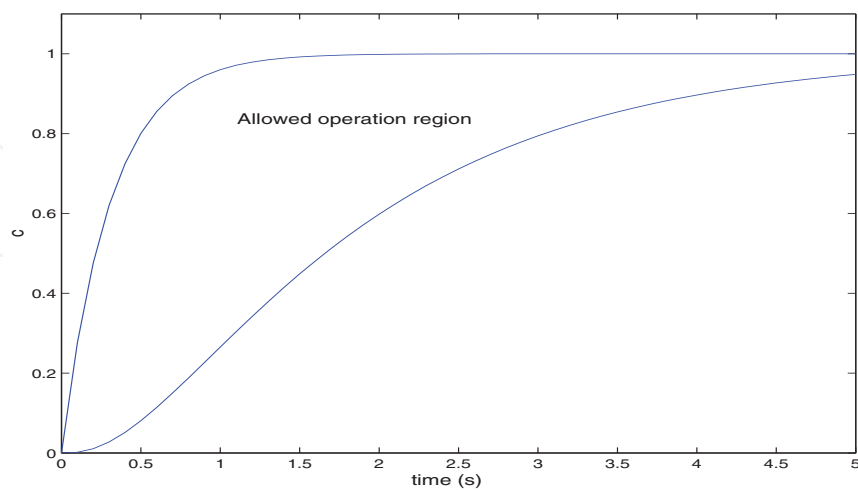
$$B_l(\omega) \leq \left| \frac{\hat{c}}{\hat{r}} \right| = \left| \frac{F(j\omega)P(j\omega)C(j\omega)}{1 + P(j\omega)C(j\omega)} \right| \leq B_u(\omega) \quad \forall \omega > 0, \forall P \in \wp \quad (5)$$



(a) Regulation problem



(b) Regulation problem for other initial conditions



(c) Tracking problem

Fig. 5. Specifications examples in time domain.

5. Noise rejection:

$$\left| \frac{\hat{c}}{\hat{n}} \right| = \left| \frac{P(j\omega)C(j\omega)}{1 + P(j\omega)C(j\omega)} \right| \leq \delta_n(\omega) \quad \forall \omega > 0, \forall P \in \wp \quad (6)$$

6. Control effort:

$$\left| \frac{\hat{u}}{\hat{n}} \right| = \left| \frac{C(j\omega)}{1 + P(j\omega)C(j\omega)} \right| \leq \delta_{ce}(\omega) \quad \forall \omega > 0, \forall P \in \wp \quad (7)$$

For specifications in Eq. (2), (3) and (5), arbitrarily small specifications can be achieved designing C so that $|C(j\omega)| \rightarrow \infty$ (due to the appearance of the M -circle in the Nichols plot). So, with an arbitrarily small deviation from the steady state, due to the disturbance, and with a sensibility close to zero, the control system is more independent of the plant uncertainty. Obviously, in order to achieve an increase in $|C(j\omega)|$ is necessary to increase the crossover frequency¹ for the system. So, to achieve arbitrarily small specifications implies to increase the bandwidth² of the system. Note that the control effort specification is defined, in this context, from the sensor noise n to the control signal u . In order to define this specification from the reference, only the closed-loop transfer function from the n signal to u signal must be multiplied by F precompensator. However, in QFT, it is not defined in this form because of F must be used with other purposes.

On the other hand, to increase the value of $|C(j\omega)|$ implies a problem in the case of the control effort specification and in the case of the sensor noise rejection, since, as was previously indicated, the bandwidth of the system is increased (so the sensor noise will affect the system performance a lot). A compromise must be achieved among the different specifications.

The stability specification is related to the relative stability margins: phase and gain margins. Hence, supposing that λ is the stability specification in Eq. (4), the phase margin is equal to $2 \cdot \arcsin(0.5\lambda)$ degrees, and the gain margin is equal to $20 \log_{10}(1 + 1/\lambda)$ dB.

The output disturbance rejection specification limits the distance from the open-loop transfer function $L(j\omega)$ to the point $(-1, 0)$ in Nyquist plane, and it sets an upper limit on the amplification of the disturbances at the plan output. So, this type of specification is also adequated for relative stability.

2.3 Translation of quantitative specifications from time to frequency domain

As was previously indicated, QFT is a frequency domain design technique, so, when the specifications are given in the time domain (typically in terms of the unit step response), it is necessary to translate them to frequency domain. One way to do it is to assume a model for the transfer function T_{cr} , closed-loop transfer function from reference r to the output c , and to find values for its parameters so that the defined time domain limits over the system output are satisfied.

2.3.1 A first-order model

Lets consider the simplest case, a first-order model given by $T_{cr}(s) = K/(s + a)$, so that when $r(t)$ is an unit step the system output is given by $c(t) = (K/a)(1 - e^{-at})$. Then, in order to reach $c(t) = r(t)$ for a time t large enough, K should be $K = a$.

¹ The crossover frequency for a system is defined as the frequency in rad/s such that the magnitude of the open-loop transfer function $L(j\omega) = P(j\omega)C(j\omega)$ is equal to zero decibels (dB).

² The bandwidth of a system is defined as the value of the frequency ω_b in rad/s such that $|T_{cr}(j\omega_b)/T_{cr}(0)|_{dB} = -3$ dB, where T_{cr} is the closed-loop transfer function from the reference r to the output c .

For a first-order model $\tau_c = 1/a = 1/\omega_b$ is the time constant (represents the time it takes the system step response to reach 63.2% of its final value). In general, the greater the bandwidth is, the faster the system output will be.

One important difficulty for a first-order model considered is that the first derivative for the output (in time infinitesimally after zero, $t = 0^+$) is $c = K$, when it would be desirable to be 0. So, problems appear at the neighborhood of time $t = 0$. In Figure 6 typical specified time limits (from Eq. (5) B_l and B_u are the magnitudes of the frequency response for these time domain limits) and the system output are shown when a first-order model is used. As observed, problems appear at the neighborhood of time $t = 0$. On the other hand the first-order model does not allow any overshoot, so from the specified time limits the first order model would be very conservative. Hence, a more complex model must be used for the closed-loop transfer function T_{cr} .

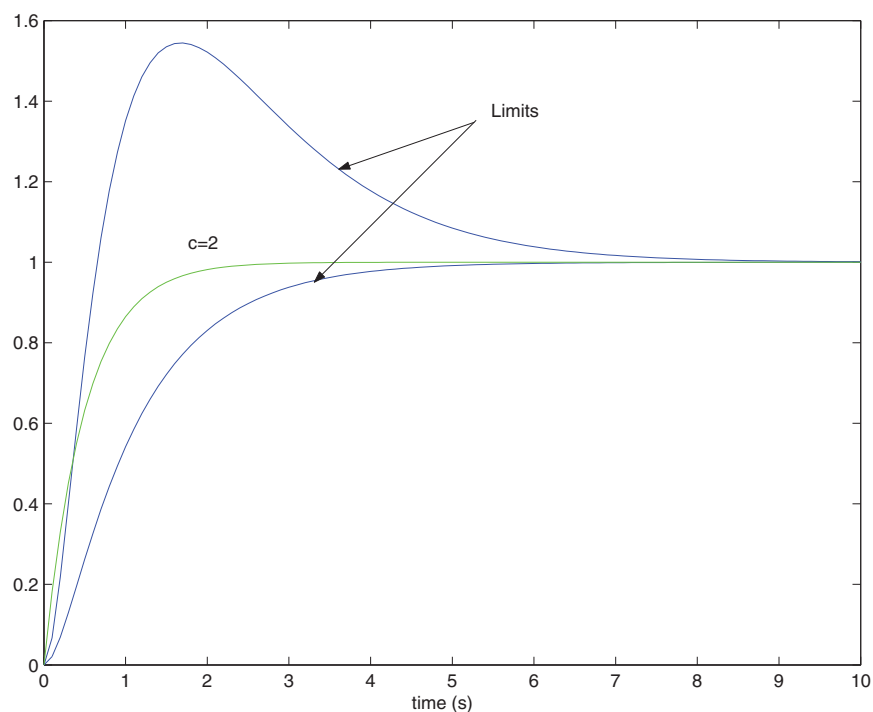


Fig. 6. Inadequate first-order model.

2.3.2 A second-order model

In this case, two free parameters are available (assuming unit static gain): the damping factor ζ and the natural frequency ω_n (rad/s). The model is given by

$$T(s) = \frac{\omega_n^2}{s^2 + 2\zeta\omega_n s + \omega_n^2} \quad (8)$$

The unit step response, depending on the value of ζ , is given by

$$c(t) = \begin{cases} 1 - e^{-\zeta\omega_n t} (\cos(\omega_n \sqrt{1 - \zeta^2} t) + \frac{\zeta\omega_n}{\omega_n \sqrt{1 - \zeta^2}} \sin(\omega_n \sqrt{1 - \zeta^2} t)) & \text{if } \zeta < 1 \\ 1 - e^{-\zeta\omega_n t} (\cosh(\omega_n \sqrt{\zeta^2 - 1} t) + \frac{\zeta\omega_n}{\omega_n \sqrt{\zeta^2 - 1}} \sinh(\omega_n \sqrt{1 - \zeta^2} t)) & \text{if } \zeta > 1 \\ 1 - e^{-\zeta\omega_n t} (1 + \omega_n t) & \text{if } \zeta = 1 \end{cases}$$

In practice, the step response for a system usually has more terms, but normally it contains a dominant second-order component with $\zeta < 1$. The second-order model is very popular in control system design in spite of its simplicity, because of it is applicable to a large number of systems. The most important time domain indexes for a second-order model are: overshoot, settling time, rise time, damping factor and natural frequency. In frequency domain, its most important indexes are: resonance peak (related with the damping factor and the overshoot), resonance frequency (related with the natural frequency), and the bandwidth (related with the rise time). The resonance peak is defined as $\max_{\omega} |T_{cr}(j\omega)| \triangleq M_p$. The resonance frequency ω_p is defined as the frequency at which $|T_{cr}(j\omega_p)| = M_p$. One way to control the overshoot is setting an upper limit over M_p . For example, if this limit is fixed on 3 dB, and the practical $T_{cr}(j\omega)$ for ω in the frequency range of interest is ruled by a pair of complex conjugated poles, then this constrain assures an overshoot lower than 27%.

In (Horowitz, 1993) tables with these relations are proposed, where, based on the experience of Professor Horowitz, makes to set a second-order model to be located inside the allowed zone defined by the possible specifications. As Horowitz suggested in his book, if the magnitude of the closed-loop transfer function T_{cr} is located between frequency domain limits $B_u(\omega)$ and $B_l(\omega)$ in Eq. (5), then the time domain response is located between the corresponding time domain specifications, or at most it would be satisfied them in a very approximated way.

2.3.3 A third-order model with a zero

A third-order model with a unit static gain is given by

$$T(s) = \frac{\mu\omega_n^3}{(s^2 + 2\zeta\omega_n s + \omega_n^2)(s + \mu\omega_n)} \quad (9)$$

For values of μ less than 5, a similar behaviour as if the pole is not added to the second-order model is obtained. So, the model in Eq. (8) would must be used.

If a zero is added to Eq. (9), it results

$$T(s) = \frac{(1 + s/\lambda\zeta\omega_n)\mu\omega_n^3}{(s^2 + 2\zeta\omega_n s + \omega_n^2)(s + \mu\omega_n)} \quad (10)$$

The unit responses obtained in this case are shown in Figure 7 for different values of λ .

As shown in Figure 7, this model implies an improvement with respect to that in Eq. (8), because of it is possible to reduce the rise time without increasing the overshoot. Obviously, if $\omega_n > 1$, then the response is ω_n times faster than the case with $\omega_n = 1$ (slower for $\omega_n < 1$). In (Horowitz, 1993), several tables are proposed relating parameters in Eq. (10) with time domain parameters as overshoot, rise time and settling time.

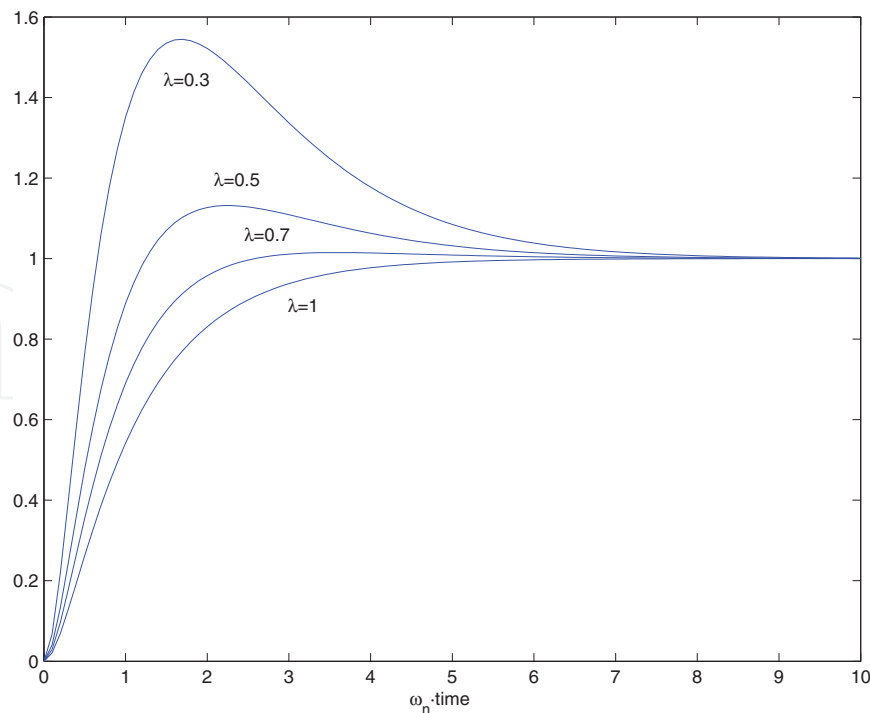


Fig. 7. Third-order model with a zero for $\mu = 5$ and $\zeta = 1$.

There exist other techniques to translate specifications from time domain to frequency domain, such as model-based techniques, where based on the structures of the plant and the controller, a set of allowed responses is defined. Another technique is that presented in (Krishnan and Cruickshanks, 1977), where the time domain specifications are formulated as $\int_0^t |c(\tau) - m(\tau)|^2 d\tau \leq \int_0^t v^2(\tau) d\tau$, with $m(t)$ and $v(t)$ specified time domain functions, and where it is established that the energy of the signal, difference between the system output and the specification $m(t)$, must be enclosed by the energy of the signal $v(t)$, for each instant t , and with a translation to the frequency domain given by the inequality $|\hat{c}(j\omega) - \hat{m}(j\omega)| \leq |\hat{v}(j\omega)|$. In (Pritchard and Wigdorowitz, 1996) and (Pritchard and Wigdorowitz, 1997), the relation time-frequency is studied when uncertainty is included in the system, so that it is possible to know the time domain limits for the system response from frequency response of a set of closed-loop transfer functions from reference to the output. This technique may be used to solve the time-frequency translation problem. However, the results obtained in translation from frequency to time and from time to frequency are very conservative.

2.4 Controller design

Now, the procedure previously introduced is explained more in detail. The aim is to design the 2DoF controller $\{F, G\}$ in Figure 1, so that a subset of specifications introduced in section 2.2 is satisfied, and the stability of the closed-loop system for all plant P in \wp is assured.

The specifications in section 2.2 are translated in circles on Nyquist plane defining allowed zones for the function $L(j\omega) = P(j\omega)C(j\omega)$. The allowed zone is the outside of the circle for specifications in Eq. (2)-(6), and the inside one for the specification in Eq. (7). Combining the allowed zones for each function L corresponding to each plant P in \wp , a set of restrictions for controller C for each frequency ω is obtained. The limits of these zones represented in Nichols

plane are called *bounds* or *boundaries*. These constraints in frequency domain can be formulated over controller C or over function $L_0 = P_0C$, for any plant P_0 in \wp (so-called nominal plant). In order to explain the detailed design process, the following example, from (Horowitz, 1993), is used. Lets suppose the plant in Figure 1 given by

$$\wp = \left\{ P(s) = \frac{k}{s(s+a)} \text{ with } k \in [1,20] \text{ and } a \in [1,5] \right\} \tag{11}$$

corresponding to a range of motors and loads, where the equation modeling the motor dynamic is $J\ddot{c} + B\dot{c} = Ku$, with $k = K/J$ and $a = B/J$ in Eq. (11). Lets suppose the tracking specifications given by

$$B_l(\omega) \leq |T_{cr}(j\omega)|_{dB} = \left| \frac{F(j\omega)P(j\omega)C(j\omega)}{1 + P(j\omega)C(j\omega)} \right|_{dB} \leq B_u(\omega) \quad \forall P \in \wp \quad \forall \omega > 0 \tag{12}$$

shown in Figure 8. In Figure 9, the difference $\delta(\omega) = B_u(\omega) - B_l(\omega)$ is shown for each frequency ω . It is easy to see that in order to satisfy the specifications in Eq. (12), the following inequality must be satisfied

$$\begin{aligned} \Delta |T_{cr}(j\omega)|_{dB} &= \max_{P \in \wp} \left| \frac{P(j\omega)C(j\omega)}{1 + P(j\omega)C(j\omega)} \right|_{dB} - \min_{P \in \wp} \left| \frac{P(j\omega)C(j\omega)}{1 + P(j\omega)C(j\omega)} \right|_{dB} \leq \\ &\leq \delta(\omega) = B_u(\omega) - B_l(\omega) \quad \forall P \in \wp \quad \forall \omega > 0 \end{aligned} \tag{13}$$

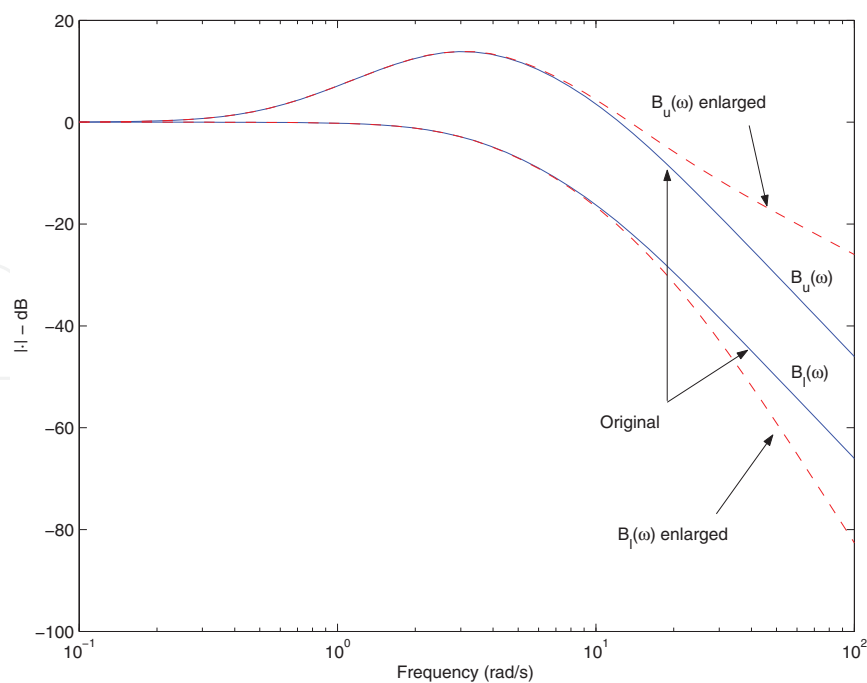


Fig. 8. Tracking specifications (variations over a nominal).

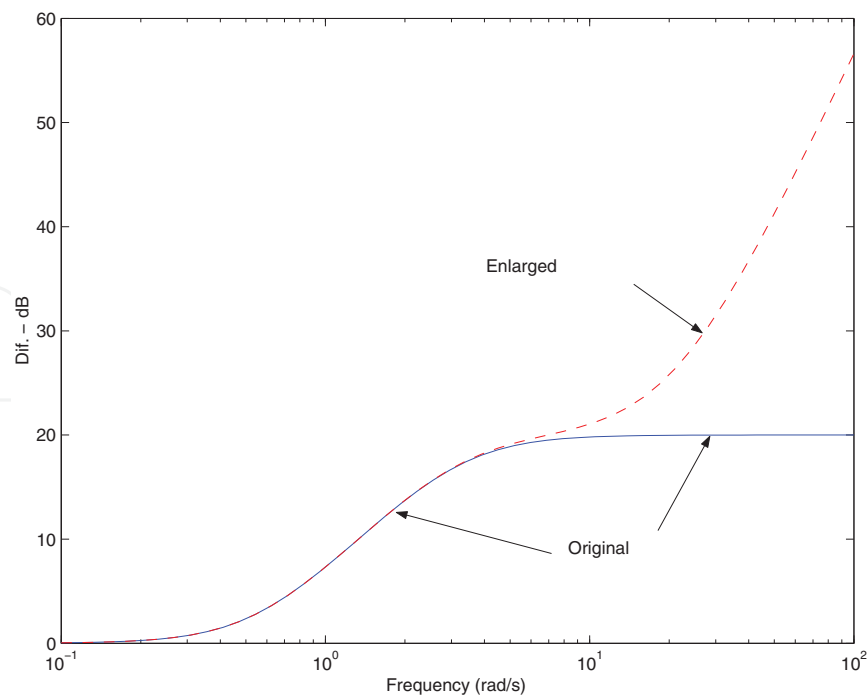


Fig. 9. Specifications on the magnitude variations for the tracking problem.

Making $L = PC$ large enough, for each plant P in \wp , and for a frequency ω , it is possible to achieve an arbitrarily small specification $\delta(\omega)$. However, this is not possible in practice, since the system bandwidth must be limited in order to minimize the influence of the sensor noise at the plant input. When C has been designed to satisfy the specifications in Eq. (13), the second degree of freedom, F , is used to locate those variations inside magnitude limits $B_l(\omega)$ and $B_u(\omega)$.

In order to design the first degree of freedom, C , it is necessary to define a set of constraints on C or on L_0 in the frequency domain, what guarantee that if C (respectively L_0) satisfies those restrictions then the specifications are satisfied too. As commented above, these constraints are called *bounds* or *boundaries* in QFT, and in order to compute them it is necessary to take into account:

- (i) A set of specifications in frequency domain, that in the case of tracking problem, are given by Eq. (13), and that in other cases (disturbance rejection, control effort, sensor noise,...) are similar as shown in section 2.2
- (ii) An object (representation) modeling the plant uncertainty in frequency domain, so-called *template*.

The following sections explain more in detail the meaning of the *templates* and the *bounds*.

Computation of basic graphical elements to deal with uncertainties: *templates*

If there is no uncertainty in plant, the set \wp would contain only one transfer function, P , and for a frequency, ω , $P(j\omega)$ would be a point in the Nichols plane. Due to the uncertainty, a set of points, for each frequency, appears in the Nichols plane. One point for each plant P in \wp . These sets are called *templates*. For example, Figure 10 shows the *template* for $\omega = 2$ rad/s, corresponding to the set:

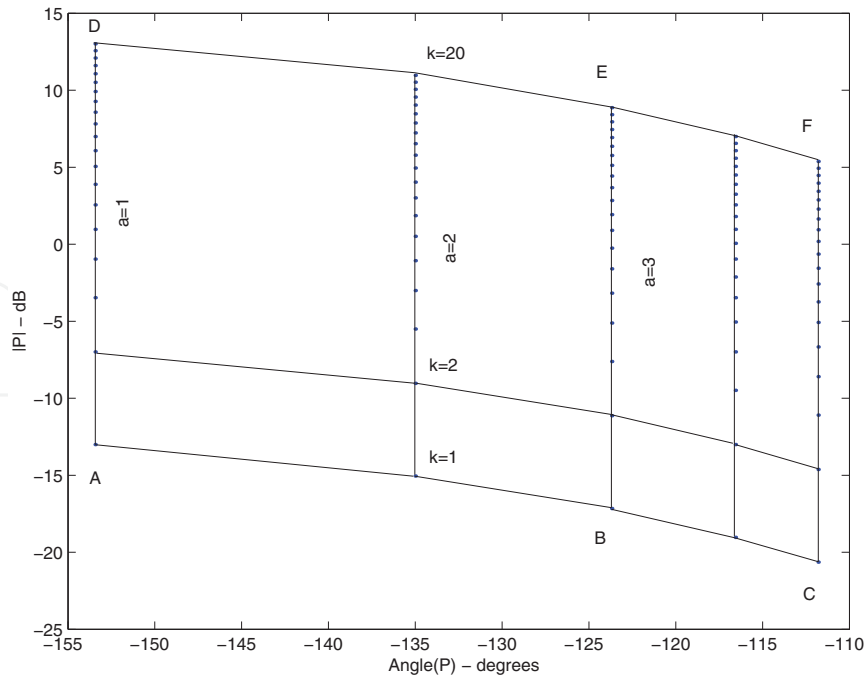


Fig. 10. Template for frequency $\omega = 2$ rad/s and the plant given by Eq. (11).

$$\mathfrak{S}(\omega = 2) = \left\{ \frac{k}{2j(2j + a)} : k \in [1, 20] \text{ and } a \in [1, 5] \right\}.$$

For $k = 1$ and driving a from 1 to 5, the segment ABC is obtained in Figure 10. For $a = 3$ and driving k from 1 to 20, the segment BE is calculated. For $k = 20$ and driving a from 1 to 5, the segment DEF is obtained.

Choosing a plant P_0 belonging to the set φ , the nominal open-loop transfer function is defined as $L_0 = P_0C$. In order to shift a template in the Nichols plane, a quantity must be added in phase (degrees) and other quantity in magnitude (decibels) to all points. Using the nominal point $P_0(j\omega)$ as representative of the full template at frequency ω and shaping the value of the nominal $L_0(j\omega) = P_0(j\omega)C(j\omega)$ using $C(j\omega)$, it is equivalent to add $|C(j\omega)|_{dB}$ in magnitude and $Angle(C(j\omega))$ degrees in phase to each point $P(j\omega)$ (with magnitude in decibels and phase in degrees) inside the template at frequency ω . So, the shaping of the nominal open-loop transfer function at frequency ω (using the degree of freedom C), is equivalent to shift the template at that frequency ω to a specific location in the Nichols plane.

The choice of the nominal plant for a template is totally free. The design method is valid independently of this choice. However, there exist rules for the more adequate choice in specific situations (Horowitz, 1993).

As was previously indicated, there exists a template for each frequency, so that after the definition of the specifications for the control problem, the following step is to define a set of design frequencies Ω . Then, the templates would be computed for each frequency ω in Ω . Once the specifications have been defined and the templates have been computed, the third step is the computation of boundaries using these graphical objects and the specifications.

Derivation of boundaries from templates and specifications

Now, zones on Nichols plane are defined for each frequency ω in Ω , so that if the nominal of the *template* shifted by $C(j\omega)$ is located inside that zone, then the specifications are satisfied.

For each specification in section 2.2 and for each frequency ω in Ω , using the *template* and the corresponding specification, the *boundary* must be computed. Details about the different types of *bounds* and the most important algorithms to compute them can be found in (Moreno et al., 2006). In general, a *boundary* at frequency ω defines a limit of a zone on Nichols plane so that if the nominal $L_0(j\omega)$ of the shifted *template* is located inside that zone, then some specifications are satisfied. So, the most single appearance of a *boundary* defines a threshold value in magnitude for each phase ϕ in the Nichols plane, so that if $\text{Angle}(L_0(j\omega)) = \phi$, then $|L_0(j\omega)|_{dB}$ must be located above (or below depending on the type of specification used to compute the *boundary*) that threshold value.

It is important to note that sometimes redefinition of the specifications is necessary. For example, for system in Eq. (11), for $\omega \geq 10$ rad/s the *templates* have similar dimensions, and the specifications from Eq. (13) in Figure 9 are identical. Then, the *boundaries* for $\omega \geq 10$ rad/s will be almost identical. The function $L_0(j\omega)$ must be above the *boundaries* for all frequencies, including $\omega \geq 10$ rad/s, but this is unviable due to it must be satisfied that $L_0(j\omega) \rightarrow 0$ when $\omega \rightarrow \infty$. Therefore, it is necessary to open the tracking specifications for high frequency (where furthermore the uncertainty is greater), such as it is shown in Figure 8. On the other hand, it must be also taken into account that for a large enough frequency ω , the specification $\delta(\omega)$ in Eq. (13) must be greater or equal than $\max_{P \in \wp} |P(j\omega)|_{dB} - \min_{P \in \wp} |P(j\omega)|_{dB}$ such that, for a small value of $L_0(j\omega)$ for these frequencies, the specifications are also satisfied. The effect of this enlargement for the specifications is negligible when the modifications are introduced at a frequency large enough. These effects are notable in the response at the neighborhood of $t = 0$.

Considering the tracking bounds as negligible from a specific frequency (in the sense that the specification is large enough), it implies that the stability boundaries are the dominant ones at these frequencies. As was mentioned above, since the templates are almost identical at high frequencies and the stability specification λ is independent of the frequency, the stability bounds are also identical and only one of them can be used as representative of the rest. In QFT, this boundary is usually called high frequency bound, and it is denoted by B_H .

Notice that the use of a discrete set of design frequencies Ω does not imply any problem. The variation of the specifications and the variation of the appearance of the *templates* from a frequency ω^- to a frequency ω^+ , with $\omega^- < \omega < \omega^+$, is smooth. Anyway, the methodology let us discern the specific cases in which the number of elements of Ω is insufficient, and let us iterate in the design process to incorporate the *boundaries* for those new frequencies, then reshaping again the compensator $\{F, C\}$.

Design of the nominal open-loop transfer function fulfilling the boundaries

In this stage, the function $L_0(j\omega)$ must be shaped fulfilling all the *boundaries* for each frequency. Furthermore, It must assure that the transfer function $1 + L(s)$ has no zeros in the right half plane for any plant P in \wp . So, initially $L_0 = P_0$ ($C = 1$) and poles and zeros are added to this function (poles and zeros of the controller C) in order to satisfy all of these restrictions on the Nichols plane. In this stage, only using the function L_0 , it is possible to assure the fulfillment of the specifications for all of the elements in the set \wp when $L_0(j\omega)$ is located inside the allowed zones defined by the *boundary* at frequency ω (computed from the corresponding *template* at that frequency, and from the specifications).

Obviously, there exists an infinite number of acceptable functions L_0 satisfying the *boundaries* and the stability condition. In order to choose among all of these functions, an important factor to be considered is the sensor noise effect at the plant input. The closed-loop transfer function from noise n to the plant input u is given by

$$T_{un}(s) = \frac{-C(s)}{1 + P(s)C(s)} = \frac{-L(s)/P(s)}{1 + L(s)}.$$

In the range of frequencies in which $|L(j\omega)|$ is large (generally low frequency), $|T_{un}(j\omega)| \rightarrow |1/P(j\omega)|$, so that the value of $|T_{un}(j\omega)|$ at low frequency is independent on the design chosen for L . In the range of frequencies where $|L(j\omega)|$ is small (generally high frequency), $|T_{un}(j\omega)| \rightarrow |G(j\omega)|$. These two asymptotes cross between themselves at the crossover frequency.

In order to reduce the influence of the sensor noise at the plant input, $|C(j\omega)| \rightarrow 0$ when $\omega \rightarrow \infty$ must be guaranteed. It is equivalent to say that $|L_0(j\omega)|$ must be reduced as fast as possible at high frequency. A conditionally stable³ design for L_0 is especially adequate to achieve this objective. However, as it is shown in (Moreno et al., 2010) this type of designs supposes a problem when there exists a saturation non-linearity type in the system.

Design of the prefilter

At this point, only the second degree of freedom, F , must be shaped. The controller C , designed in the previous step, only guarantees that the specifications in Eq. (13) are satisfied, but not the specifications in Eq. (12). Using F , it is possible to guarantee that the specifications in Eq. (12) are satisfied when with C the specifications in Eq. (13) are assured.

In order to design F , the most common method consists of computing for each frequency ω the following limits

$$F_u(\omega) = \left| \max_{P \in \varphi} \left| \frac{P(j\omega)C(j\omega)}{1 + P(j\omega)C(j\omega)} \right|_{dB} - B_u(\omega) \right|$$

and

$$F_l(\omega) = \left| \min_{P \in \varphi} \left| \frac{P(j\omega)C(j\omega)}{1 + P(j\omega)C(j\omega)} \right|_{dB} - B_l(\omega) \right|$$

and shaping F adding poles and zeros until $F_l(\omega) \leq |F(j\omega)| \leq F_u(\omega)$ for all frequency ω in Ω .

Validation of the design

This is the last step in the design process and consists in studying the magnitude of the different closed-loop transfer functions, checking if the specifications for frequencies outside of the set Ω are satisfied. If any specification is not satisfied for a specific frequency, ω_p , then this frequency is added to the set Ω , and the corresponding *template* and *boundary* are

³ A system is conditionally stable if a gain reduction of the open-loop transfer function L drives the closed-loop poles to the right half plane.

computed for that frequency ω_p . Then, the function L_0 is reshaped, so that the new restriction is satisfied. Afterwards, the precompensator F is reshaped, and finally the new design is validated. So, an iterative procedure is followed until the validation result is satisfactory.

3. Computer-based tools for QFT

As it has been described in the previous section, the QFT framework evolves several stages, where a continuous re-design process must be followed. Furthermore, there are some steps requiring the use of algorithms to calculate the corresponding parameters. Therefore, computer-based tools as support for the QFT methodology are highly valuable to help in the design procedure. This section briefly describes the most well-known tools available in the literature, The Matlab QFT Toolbox (Borghesani et al., 2003) and SISO-QFTIT (Díaz et al., 2005a),(Díaz et al., 2005b).

3.1 Matlab QFT toolbox

The QFT Frequency Domain Control Design Toolbox is a commercial collection of Matlab functions for designing robust feedback systems using QFT, supported by the company Terasoft, Inc (Borghesani et al., 2003). The QFT Toolbox includes a convenient GUI that facilitates classical loop shaping of controllers to meet design requirements in the face of plant uncertainty and disturbances. The interactive GUI for shaping controllers provides a point-click interface for loop shaping using classical frequency domain concepts. The toolbox also includes powerful *bound* computation routines which help in the conversion of closed-loop specifications into *boundaries* on the open-loop transfer function (Borghesani et al., 2003).

The toolbox is used as a combination of Matlab functions and graphical interfaces to perform a complete QFT design. The best way to do that is to create a Matlab script including all the required calls to the corresponding functions. The following lines briefly describe the main steps and functions to use, where an example presented in (Borghesani et al., 2003) is followed for a better understanding (a more detailed description can be found in (Borghesani et al., 2003)).

The example to follow is described by:

$$\wp = \left\{ P(s) = \frac{k}{(s+a)(s+b)} : k = [1, 2, 5, 8, 10], a = [1, 3, 5], b = [20, 25, 30] \right\}. \quad (14)$$

Once the process and the associated uncertainties are defined, the different steps, explained in section 2, to design the robust control scheme using the QFT toolbox are described in the following:

- *Template computation.* First, the transfer function models representing the process uncertainty must be written. The following code calculates a matrix of 40 plant elements which is stored in the variable P and represents the system defined by Eq. (14).
 - » $c = 1; k = 10; b = 20;$
 - » for $a = \text{linspace}(1,5,10),$
 - » $P(1,1,c) = \text{tf}(k,[1,a+b,a*b]); c = c + 1;$
 - » end
 - » $k = 1; b = 30;$
 - » for $a = \text{linspace}(1,5,10),$

```

» P(1,1,c) = tf(k,[1,a+b,a*b]); c = c + 1;
» end
» b = 30; a = 5;
» for k = linspace(1,10,10),
»     P(1,1,c) = tf(k, [1,a+b,a*b]); c = c + 1;
» end
» b = 20; a = 1;
» for k = linspace(1,10,10),
»     P(1,1,c) = tf(k, [1,a+b,a*b]); c = c + 1;
» end

```

Then, the nominal element is selected:

```
» nompt=21;
```

and the frequency array is set:

```
» w = [0.1, 5, 10, 100];
```

Finally, the templates are calculated and visualized using the *plottmpl* function (see (Borghesani et al., 2003) for a detailed explanation):

```
» plottmpl(w,P,nompt);
```

obtaining the *templates* shown in Figure 11.

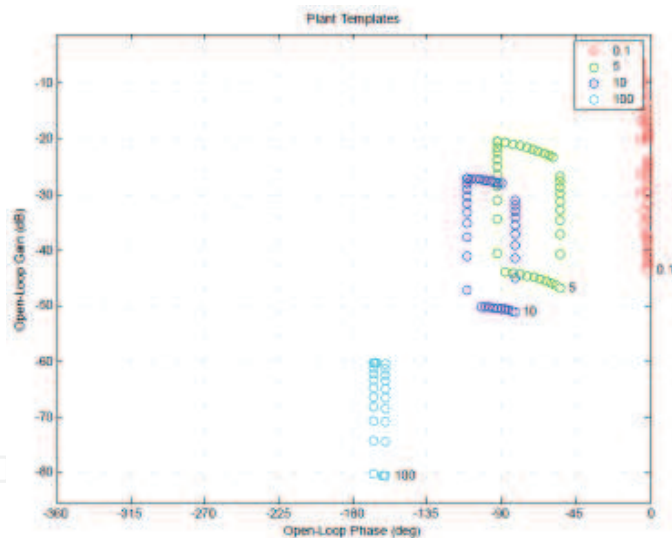


Fig. 11. Matlab QFT Toolbox. Templates for example in Eq. (14)

- *Specifications.* In this step, the system specifications must be defined according to Eq. (2)-(7). Once the specifications are determined, the corresponding bounds on the Nichols plane are computed. The following source code shows the use of specifications in Eq. (2)-(4) for this example.

A stability specification of $\lambda = 1.2$ in Eq. (4) corresponding to a gain margin (GM) ≥ 5.3 dB and a phase margin (PM) = 49.25 degrees is given:

```
» Ws1 = 1.2;
```

Then, the stability *bounds* are computed using the function *sisobnds* (see (Borghesani et al., 2003) for a detailed explanation) and its value is stored in the variable *bdb1*:

```
» bdb1 = sisobnds(1,w,Ws1,P,0,nompt);
```

Lets now consider the specifications for output and input disturbance rejection cases, from Eq. (2)-(3). For the case of the output disturbance specification, the performance weight for the bandwidth [0,10] is defined as

```
» Ws2 = tf(0.02*[1,64,748,2400],[1,14.4,169]);
```

and the *bounds* are computed in the following way

```
» bdb2 = sisobnds(2,w(1:3),Ws2,P,0,nompt);
```

For the input disturbance case, the specification is defined as constant for

```
» Ws3 = 0.01;
```

calculating the *bounds* as

```
» bdb3 = sisobnds(3,w(1:3),Ws3,P,0,nompt);
```

also for the bandwidth [0,10].

Once the specifications are defined and the corresponding *bounds* are calculated. For each frequency they can be combined using the following functions:

```
» bdb = grpbnds(bdb1,bdb2,bdb3); // Making a global structure
```

```
» ubdb = sectbnds(bdb); // Combining bounds
```

The resulting *bounds* which will be used for the loop-shaping stage are shown in Figure 12. This figure is obtained using the *plotbnds* function:

```
» plotbnds(ubdb);
```

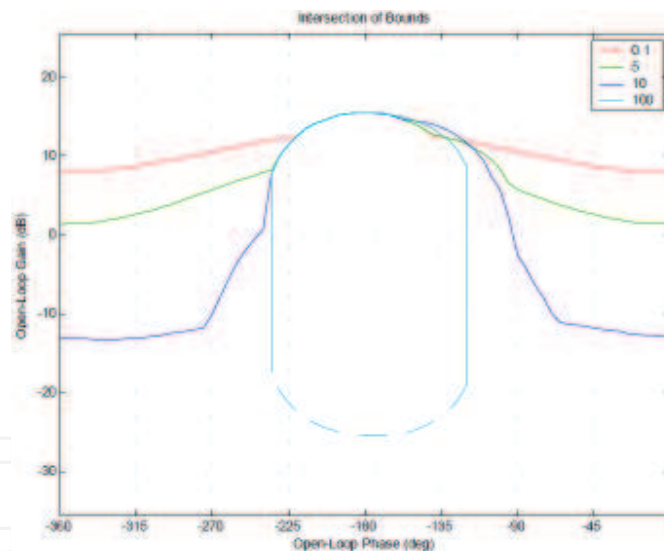


Fig. 12. Matlab QFT Toolbox. Boundaries for example (14)

- *Loop-shaping*. After obtaining the stability and performance *bounds*, the next step consists in designing (loop shaping) the controller. The QFT toolbox includes a graphical interactive GUI, *lpshape*, which helps to perform this task in an straightforward way. Before using this function, it is necessary to define the frequency array for loop shaping, the nominal plant, and the initial controller transfer function. Therefore, these variables must be set previously, where for this example are given by:

```
» wl = logspace(-2,3,100); // frequency array for loop shaping
```

```
» C0 = tf(1,1); // Initial Controller
```

» L0=P(1,1,nompt)*C0; // Nominal open-loop transfer function

Having defined these variables, the graphical interface is opened using the following line:

» lpshape(wl,ubdb,L0,C0);

obtaining the window shown in Figure 13. As shown from this figure, the GUI allows to modify the control transfer functions adding, modifying, and removing poles and zeros. This task can be done from the options available at the right area of the windows or dragging interactively on the loop $L_0(s) = P_0(s)C(s)$ represented by the black line on the Nichols plane.

For this example, the final controller is given by (Borghesani et al., 2003)

$$C(s) = \frac{379\left(\frac{s}{42} + 1\right)}{\frac{s^2}{247^2} + \frac{s}{247} + 1} \quad (15)$$

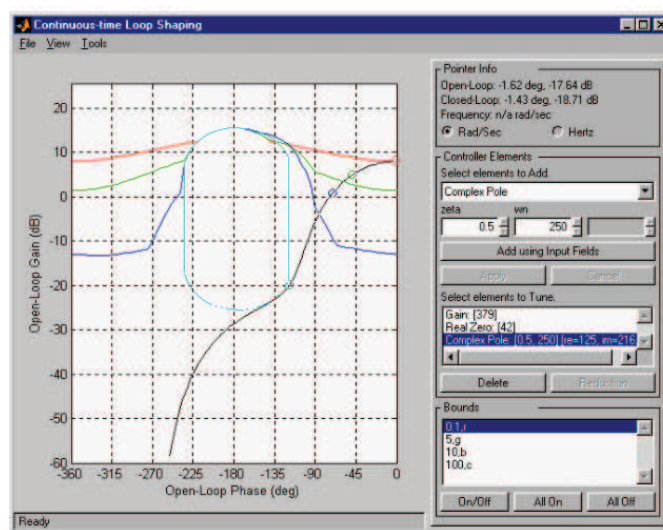


Fig. 13. Matlab QFT Toolbox. Loop shaping for example in Eq. (14)

- *Pre-filter design.* When the control design requires tracking of reference signals, although this is not the case for this example, a pre-filter $F(s)$ must be used in addition to the controller $C(s)$ such as discussed in section 2.. The prefilter can be also designed interactively using a graphical interface similar to that described for the loop shaping stage. To run this option, the *pfshape* function must be used (see (Borghesani et al., 2003) for more details).
- *Validation.* The control system validation can be done testing the resulting robust controller for all uncertain plants defined by Eq. (14) and checking that the different specifications are fulfilled for all of them. This task can be performed directly programming in Matlab or using the *chksiso* function from the QFT toolbox.

3.2 An interactive tool based in Sysquake: SISO-QFTIT

SISO-QFTIT is a free software interactive tool for robust control design using the QFT methodology (Díaz et al., 2005a;b). The main advantages of SISO-QFTIT compared to other existing tools are its easiness of use and its interactive nature. In the tool described in the previous section, a combination between code and graphical interfaces must be used, where

some interactive features are also provided for the loop shaping and filter design stages. However, with SISO-QFTIT all the stages are available from an interactive point of view.

As commented above, the tool has been implemented in Sysquake, a Matlab-like language with fast execution and excellent facilities for interactive graphics (Piguet, 2004). Windows, Mac, and Linux operating systems are supported. Since this tool is completely interactive, one consideration that must be kept in mind is that the tool's main feature -interactivity- cannot be easily illustrated in a written text. Thus, the reader is cordially invited to experience the interactive features of the tool.

The users mainly should operate with only mouse operations on different elements in the window of the application or text insertion in dialog boxes. The actions that they carry out are reflected instantly in all the graphics in the screen. In this way the users take aware visually of the effects that produce their actions on the design that they are carrying out. This tool is specially conceived as much as for beginner users that want to learn the QFT methodology, as for expert users (Díaz et al., 2005b).

The user can work with SISO-QFTIT in two different but not excluding ways (Díaz et al., 2005b):

- Interactive mode. In this work form, the user selects an element in the window and drags it to take it to a certain value, their actions on this element are reflected simultaneously on all the present figures in the window of the tool.
- Dialogue mode. In this work form, the user should simply go selecting entrances of the *Settings* menu and correctly fill the blanks of dialog boxes.

Such as commented in the manual of this interactive software tool, its main interactive advantages and options are the following (Díaz et al., 2005b):

- Variations that take place in the *templates* when modifying the uncertainty of the different elements of the plant or in the value of the *template* calculation frequency.
- Individual or combined variation on the bounds as a result of the configuration of specifications, i.e., by adding zeros and poles to the different specifications.
- The movement of the controller zeros and poles over the complex plane and the modification of its symbolic transfer function when the open loop transfer function is modified in the Nichols plane.
- The change of shape of the open loop transfer function in the Nichols plane and the variation of the expression of the controller transfer function when any movement, addition or suppression of its zeros or poles in the complex plane.
- The changes that take place in the time domain representation of the manipulated and controlled variables due to the modification of the nominal values of the different elements of the plant.
- The changes that take place in the time domain representation of the manipulated and controlled variables due to the introduction of a step perturbation at the input of the plant. The magnitude and the occurrence instant of the perturbation is configured by the user by means of the mouse.

Such as pointed out above, the interactive capabilities of the tool cannot be shown in a written text. However, some screenshots for the example used with the Matlab QFT toolbox are provided. Figure 14a shows the resulting templates for the process defined by Eq. (14).

Notice that with this tool, the frequencies, the process uncertainties and the nominal plant can be interactively modified. The stability bounds are shown in Figure 14b. The radiobuttons available at the top-right side of the tool allow to choose the desired specification. Once the specification is selected, the rest of the screen is changed to include the specification values in an interactive way. Figure 15a displays the loop shaping stage with the combination of the different bounds (same result than in Figure 13). The figure also shows the resulting loop shaping for controller (15). Then, the validation screen is shown in Figure 15b, where it is possible to check interactively if the robust control design satisfies the specifications for all uncertain cases. Although for this example it is not necessary to design the pre-filter for the tracking specifications, this tool also provides a screen where it is possible to perform this task (see an example in Figure 16).

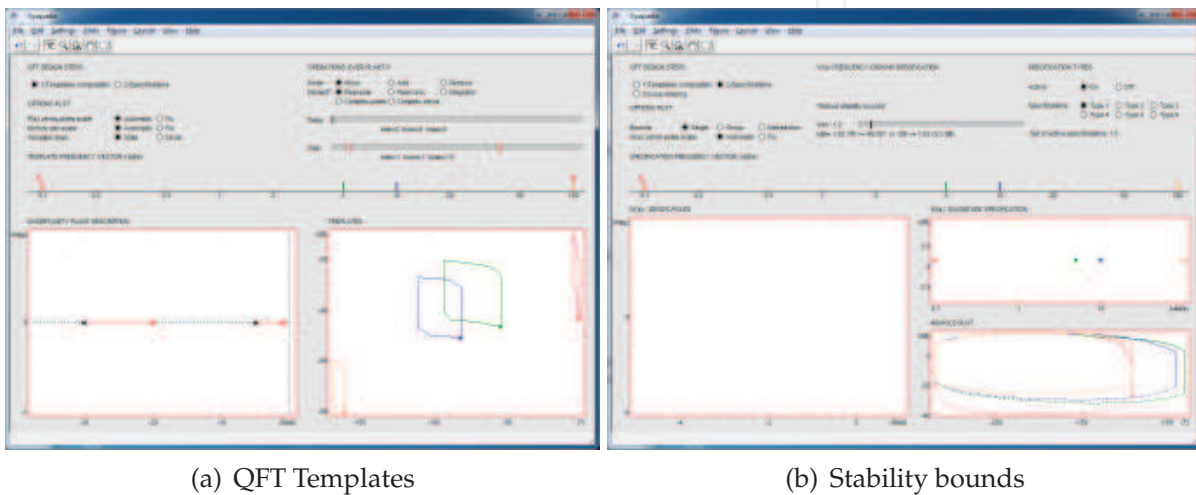


Fig. 14. SISO-QFTIT. Templates and bounds for the example described in Eq. (14)

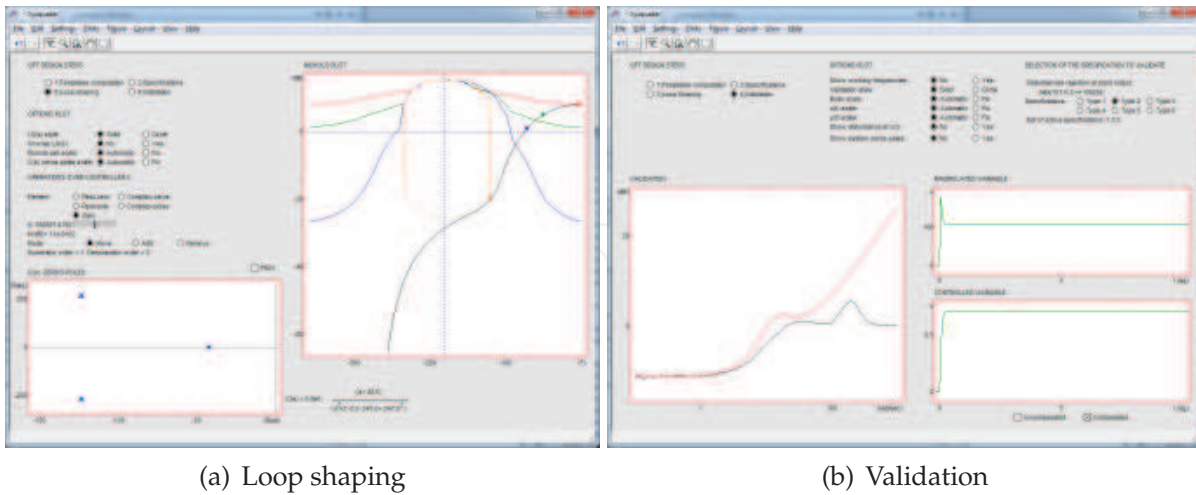


Fig. 15. SISO-QFTIT. Loop shaping and validation for the example described in Eq. (14)

4. Practical applications

This section presents two industrial projects where the QFT technique has been successfully used. The first one is focused on the pressure control of a mobile robot which was design

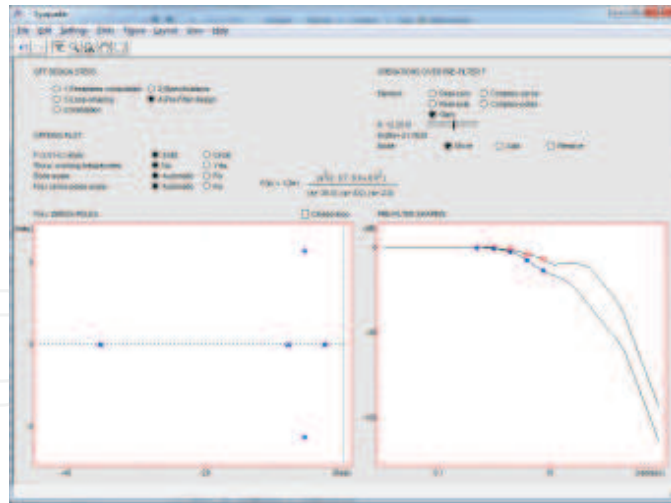


Fig. 16. SISO-QFTTIT. Prefilter stage

for spraying tasks in greenhouses (Guzmán et al., 2008). The second one deals with the temperature control of a solar collector field (Cirre et al., 2010).

4.1 In agricultural and robotics context: Fitorobot

During the last six years, the Automatic Control, Robotics and Electronics research group and the Agricultural Engineering Department, both from the University of Almería (Spain), have been working in a project aimed at designing, implementation, and testing a multi-use autonomous vehicle with safe, efficient, and economic operation which moves through the crop lines of a greenhouse and which performs tasks that are tedious and/or hazardous for people. This robot has been called *Fitorobot*. The first version of this vehicle has been equipped for spraying activities, but other configurations have also been designed, such as: a lifting platform to reach high zones to perform tasks (staking, cleaning leaves, harvesting, manual pollination, etc.), and a forklift to transport and raise heavy materials (Sánchez-Gimeno et al., 2006). This mobile robot was designed and built following the paradigm of Mechatronics such as described in (Sánchez-Hermosilla. et al., 2010).

The first objective of the project consisted of developing a prototype to enable the spraying of a certain volume of chemical products per hectare while controlling the different variables that affect the spraying system (pressure, flow, and travel speed). The pressure is selected and the control signal keeps the spraying conditions constant (mainly droplet size). The reference value of the pressure is calculated based on the mobile robot speed and the volume of pesticide to apply, where the pressure working range is between 5 and 15 bar.

There are some circumstances where it is impossible to maintain a constant velocity due to the irregularities of the soil, different slopes of the ground, and the turning movements between the crop lines. Thus, for work at a variable velocity (Guzmán et al., 2008), it is necessary to spray using a variable-pressure system based on the vehicle velocity, which is the proposal adopted and implemented in this work. This system presents some advantages, such as the higher quality of the process, because the product sprayed over each plant is optimal. Furthermore, this system saves chemical products because an optimal quantity is sprayed, reducing the environmental impact and pollution as the volume sprayed to the air is minimized.

The robot prototype (Figure 17) consists of an autonomous mobile platform with a rubber tracked system and differential guidance mechanism (to achieve a more homogeneous

distribution of soil-compaction pressure, thus disturbing less the sandy soil typical of Mediterranean greenhouses (Sánchez-Gimeno et al., 2006)). The robot is driven by hydraulic motors fed by two variable displacement pumps powered by a 20-HP gasoline motor, allowing a maximum velocity of 2.9 m/s. Due to the restrictions imposed by the narrow greenhouse lanes, the vehicle dimensions are 70 cm width, 170 cm length, and 180 cm height at the top of the nozzles.



Fig. 17. Mobile robot for agricultural tasks

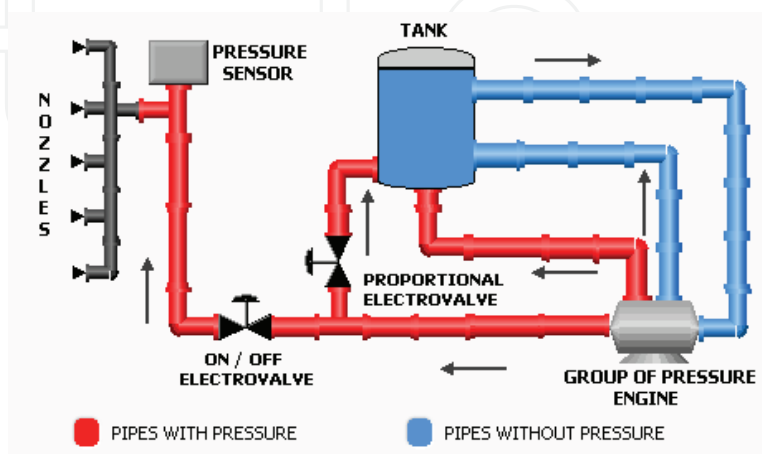


Fig. 18. Scheme of the spraying system

The spraying system carried out by the mobile robot is composed with a 300 l tank used to store the chemical products, a vertical boom sprayer with 10 nozzles, an on/off electrovalve to activate the spraying, a proportional electrovalve to regulate the output pressure, a double-membrane pump with pressure accumulator providing a maximum flow of 30 l/min and a maximum pressure of 30 bar, and a pressure sensor to close the control loop as shown in Figure 18.

In this case, the control problem was focused on regulating the output pressure of the spraying system mounted on the mobile robot despite changes in the vehicle velocity and the nonlinearities of the process.

For an adequate control system design, it was necessary to model the plant by obtaining its associated parameters. Several open-loop step-based tests were performed varying the valve aperture around a particular operating point. The results showed that the system dynamics can be approximated by a first-order system with delay. Thus, it can be modelled using the following transfer function

$$P(s) = \frac{k}{\tau s + 1} e^{-t_r s} \quad (16)$$

where k is the static gain, t_r is the delay time, and τ is the time constant.

Then, several experiments in open loop were performed to design the dynamic model of the spraying system using different amplitude opening steps (5% and 10%) over the same operating points (see Figure 19a). The analysis of the results showed that the output-pressure behavior changes when different valve-amplitude steps are produced around the same working point, and also when the same valve opening steps are produced at several operating points, confirming the uncertainty and nonlinear characteristics of the system.

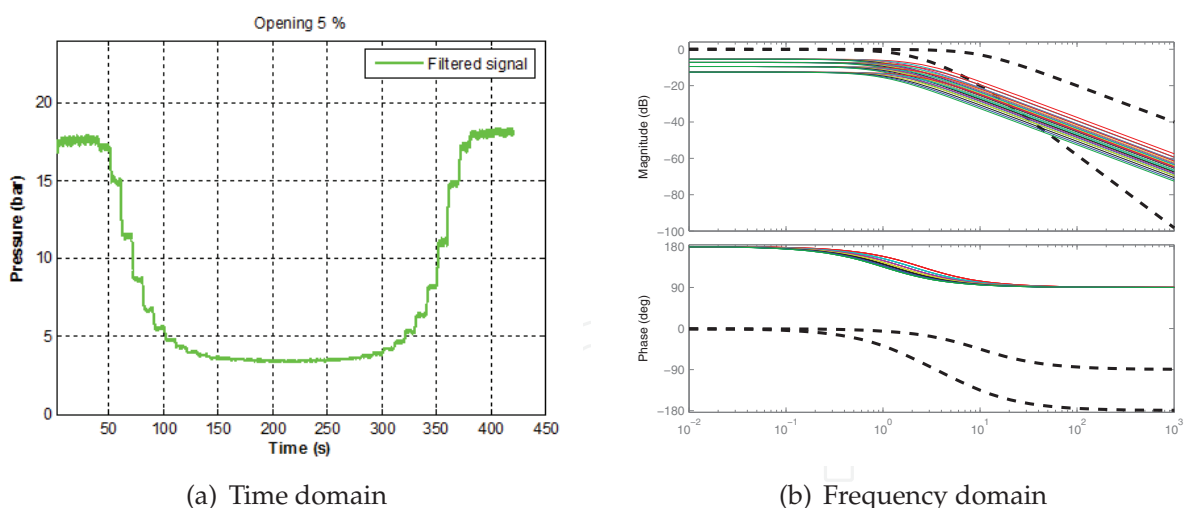


Fig. 19. System uncertainties from the time and frequency domains

After analyzing the results (see Figure 19a), the system was modelled as a first-order dynamical system with uncertain parameters, where the reaction curve method has been used at the different operating points. Therefore, the resulting uncertain model is given by the following transfer function (see Figure 19b):

$$\varphi = \left\{ P(s) = \frac{k}{\tau s + 1} : k \in [-0.572, -0.150], \tau \in [0.4, 1] \right\} \quad (17)$$

where the gain, k , is given in bar/% aperture and the constant time, τ , in seconds. Once the system was characterized, the robust control design using QFT was performed considering specifications on stability and tracking.

First, the specifications for each frequency were defined, and the nominal plant P_0 was selected. The set of frequencies and the nominal plant were set to $\Omega = \{0.1, 1, 2, 10\}$ rad/s and $P_0 = \frac{-0.3}{0.7s+1}$, respectively. The stability specification was set to $\lambda = 1.2$ corresponding to a $GM \geq 5.3$ dB and a $PM = 49.25$, and for the tracking specifications the maximum and minimum values for the magnitude have been described by the following transfer functions (frequency response for tracking specifications are shown in Figure 19b in dashed lines)

$$B_l(s) = \frac{10}{s + 10}, \quad B_u(s) = \frac{12.25}{s^2 + 8.75s + 12.25} \tag{18}$$

Figure 20a shows the different *templates* of the plant for the set of frequencies determined above.

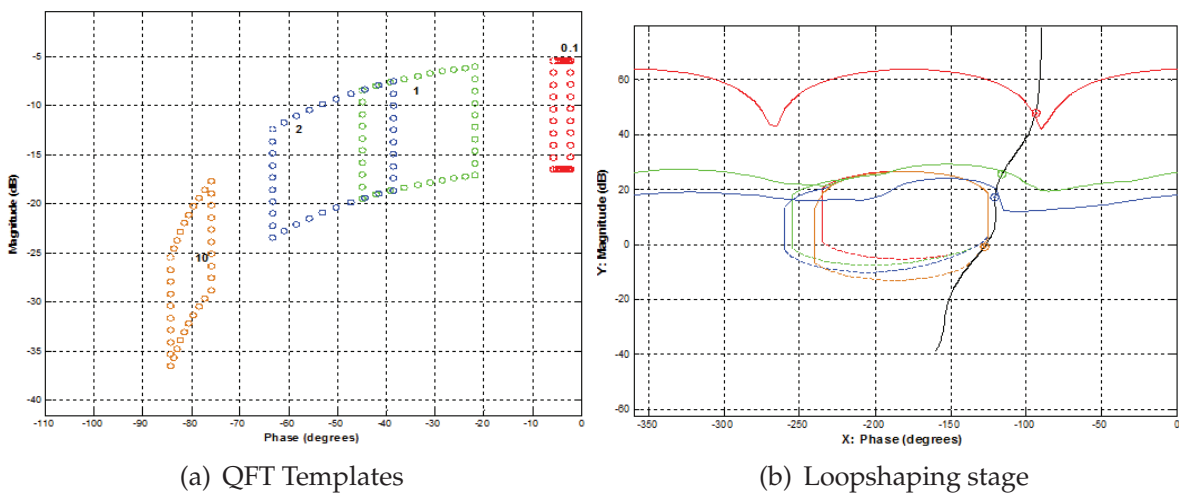


Fig. 20. Templates and feedback controller design by QFT

The specifications are translated to the *boundaries* on the Nichols plane for the loop-transfer function $L(j\omega) = C(j\omega)P(j\omega)$. Figure 20b shows the different *bounds* for stability and tracking specifications set previously.

Then, the loop shaping stage was performed in such a way that the nominal loop-transfer function $L_0(j\omega) = C(j\omega)P_0(j\omega)$ was adjusted to make the templates fulfil the *bounds* calculated in the previous phase. Figure 20b shows the design of L_0 where the *bounds* are fulfilled at each design frequency. This figure shows the optimal controller using QFT to lie on the *boundaries* at each frequency design. However, a simpler controller fulfilling the specifications was preferred for practical reasons. The resulting controller was the following:

$$C(s) = \frac{27.25(s + 1)}{s} \tag{19}$$

To conclude the design process, the prefilter F is determined so that the closed-loop transfer function matches the robust tracking specifications, that is, the closed-loop system variations must be inside of a desired tolerance range:

$$F(s) = \frac{1}{0.1786s + 1} \tag{20}$$

Once the robust design was performed, the system was validated by simulation. Figure 21 shows the validation results where the specifications are clearly satisfied for the whole family of plants described by Eq. (17) for the time domain and frequency domain, respectively.

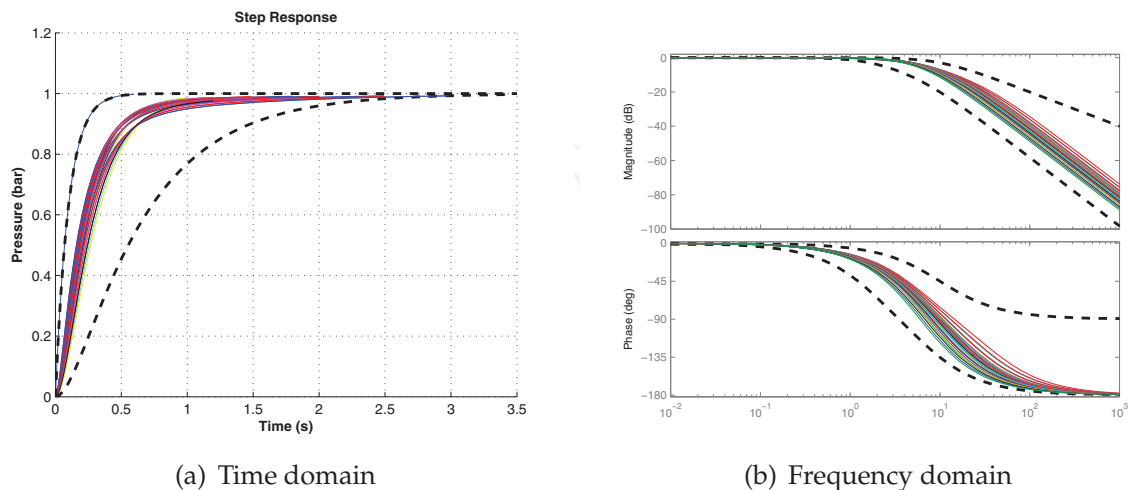


Fig. 21. Validation for the QFT design of the pressure system

If the results shown in Figure 19b are compared with those shown in Figure 21b, a considerable uncertainty reduction can be appreciated, especially in the gain system. Notice that Figure 19 shows the responses of the open-loop system against step inputs for the time and frequency domains, respectively. From these figures, the system uncertainties can be observed by deviations in the static gain and in the time constant of the system, such as described in equation (17).

Finally, the proposed control scheme was tested on the spraying system. The robust control system is characterized by the ability of the closed-loop system to reach desired specifications satisfactorily despite of large variations in the (open-loop) plant dynamics. As commented above, in the pressure system presented in this work such variations appear along the different operating points of the process. Therefore, the system was initially tested through a group of different steps in order to verify that the control system fulfills the robust specifications. Figure 22 shows the results for a sequence of typical steps. It can be observed that the system faithfully follows the proposed reference, reaching the same performance for the different operating points.

4.2 In solar energy field: ACUREX

This section presents a robust control scheme for a distributed solar collector (DSC) field. As DSC are systems subjected to strong disturbances (mainly in solar radiation and inlet oil temperature), a series feedforward was used as a part of the plant, so that the system to be controlled has one input (fluid flow) and one output (outlet temperature) as the disturbances are partially compensated by the series feedforward term, so that the nonlinear plant is transformed into an uncertain linear system. The QFT technique (QFT) was used to design a control structure that guarantee desired control specifications, as settling time and maximum overshoot, under different operating conditions despite system uncertainties and disturbances (Cirre et al., 2010).

The main difference between a conventional power plant and a solar plant is that the primary energy source, while being variable, cannot be manipulated. The objective of the

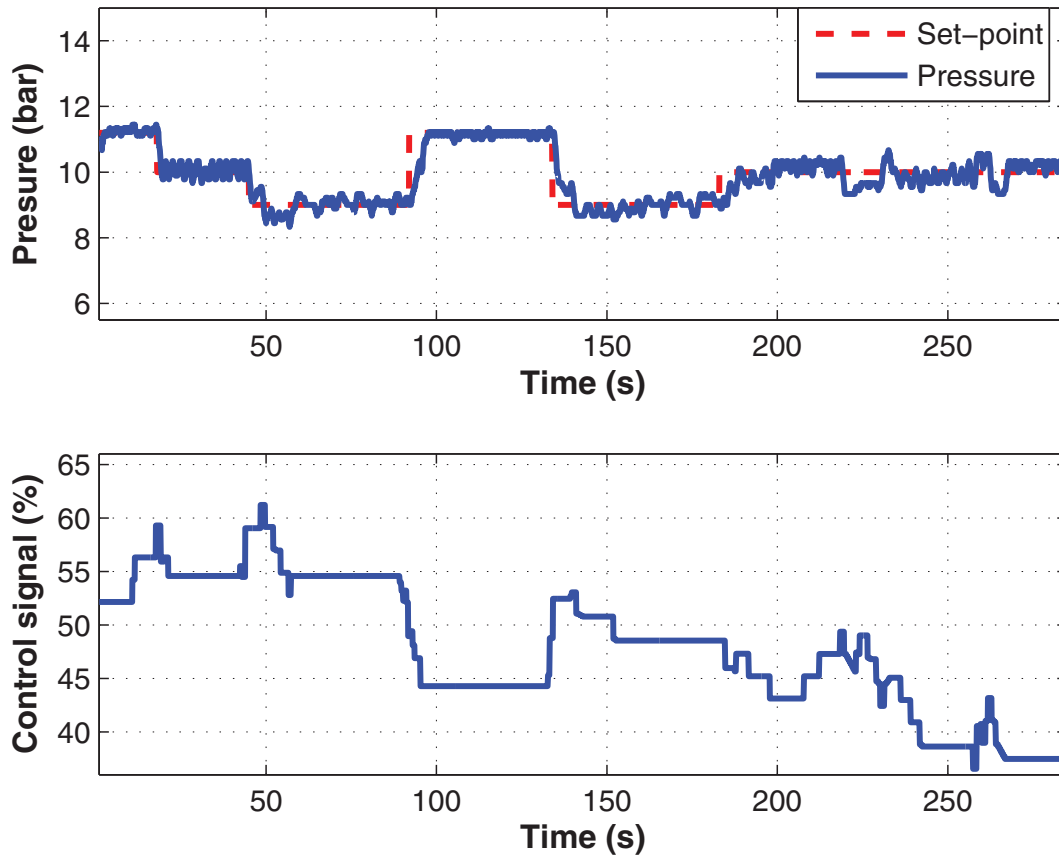


Fig. 22. Experimental tests for the spraying system

control system in a distributed solar collector field (DCS) is to maintain the outlet oil temperature of the loop at a desired level in spite of disturbances such as changes in the solar irradiance level (caused by clouds), mirror reflectivity, or inlet oil temperature. The means available for achieving this is via the adjustment of the fluid flow and the daily solar power cycle characteristics are such that the oil flow has to change substantially during operation. This leads to significant variations in the dynamic characteristics of the field, which cause difficulties in obtaining adequate performance over the operating range with a fixed parameter controller (Camacho et al., 1997; 2007a;b). For that reason, this section summarizes a work developed by the authors where a robust PID controller is designed to control the outlet oil temperature of a DSC loop using the QFT technique.

In this work, the ACUREX thermosolar plant was used, which is located at the Plataforma Solar de Almería (PSA), a research centre of the Spanish Centro de Investigaciones Energéticas Medioambientales y Tecnológicas (CIEMAT), in Almería, Spain. The plant is schematically composed of a distributed collector field, a recirculation pump, a storage tank and a three-way valve, as shown in Figures 23 and 24. The distributed collector field consists of 480 east-west-aligned single-axis-tracking parabolic trough collectors, with a total mirror aperture area of 2672 m², arranged in 20 rows forming 10 parallel loops (see Figure 23). The parabolic mirrors in each collector concentrate the solar irradiation on an absorber tube through which Santotherm 55 heat transfer oil is flowing. For the collector to concentrate sunlight on its focus, the direct solar radiation must be perpendicular to the mirror plane. Therefore, a sun-tracking

algorithm causes the mirrors to revolve around an axis parallel to the tube. Oil is recirculated through the field by a pump that under nominal conditions supplies the field at a flow rate of between 2 l/s (in some applications 3 l/s) and 12 l/s. As it passes through the field, the oil is heated and then the hot oil enters a thermocline storage tank, as shown in Figure 24. A complete detailed description of the ACUREX plant can be found in (Camacho et al., 1997).



Fig. 23. ACUREX solar plant

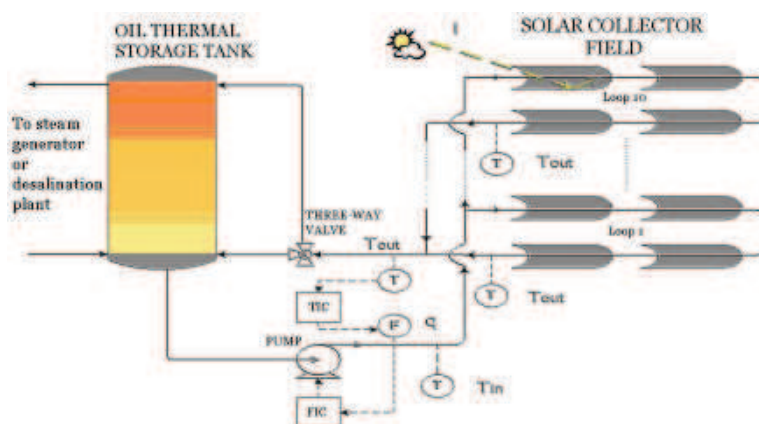


Fig. 24. Simplified layout of the ACUREX plant

As described in (Camacho et al., 1997), DSC dynamics can be approximated by low-order linear descriptions of the plant (as is usually done in the process industry) to model the system around different operating conditions and to design diverse control strategies without accounting for system resonances (Álvarez et al., 2007; Camacho et al., 1997). Thus, different low-order models are found for different operating points mainly due to fluid velocity and system disturbances. Using the series feedforward controller (presented in (Camacho et al., 1997) and improved in (Roca et al., 2008)), a nonlinear plant subjected to disturbances is treated as an uncertain linear plant with only one input (the reference temperature to the feedforward controller, T_{rff}).

After performing an analysis of the frequency response (Berenguel et al., 1994), it was observed that the characteristics of the system (time constants, gains, resonance modes, ...) depend on the fluid flow rate as expected (Álvarez et al., 2007; Camacho et al., 1997). Therefore, in order to control the system with a fixed-parameter controller, the following model has been used

$$\varphi = \left\{ P(s) = \frac{k\omega_n^2}{s^2 + 2\zeta\omega_n s + \omega_n^2} e^{-\tau_d s} : \zeta = 0.8, \right. \quad (21)$$

$$\left. \tau_d = 39s, \omega_n \in [0.0038, 0.014] \text{rad/s}, k \in [0.7, 1.05] \right\},$$

where the chosen nominal plant is $P_0(s)$ with $\omega_n = 0.014$ rad/s and $k = 0.7$.

Thus, once the uncertain model has been obtained, the specifications were determined on time domain and translated into the frequency domain for the QFT design. In this case, the tracking and stability specifications were established (Horowitz, 1993). For tracking specifications only is necessary to impose the minimum and maximum values for the magnitude of the closed-loop transfer function from the reference input to the output in all frequencies. With respect to the stability specification, the desired gain (GM) and phase (PM) margins are set.

The tracking specifications were required to fulfill a settling time between 5 and 35 minutes and an overshoot less than 30% after 10-20°C setpoint changes for all operating conditions (realistic specifications, see (Camacho et al., 2007a;b)).

For stability specification, $\lambda = 3.77$ in Eq. (4) is selected in order to guarantee at least a phase margin of 35 degrees for all operating conditions.

To design the compensator $C(s)$, the tracking specifications in Eq. (13), shown in Table 1 for each frequency in the set of design frequencies Ω , are used

Table 1. Tracking specifications for the C compensator design

ω (rad/s)	0.0006	0.001	0.003	0.01
$\delta(\omega)$	0.55	1.50	9.01	19.25

The resulting compensator $C(s)$, synthesized in order to achieve the stability specifications and the tracking specifications previously indicated, is the following PID-type controller

$$C(s) = 0.75 \left(1 + \frac{1}{180s} + 40s \right) \quad (22)$$

which represents the resulting loop shaping in Figure 25.

Then, in order to satisfy the tracking specifications, the prefilter $F(s)$ must be designed, where the synthesized prefilter is given by

$$F(s) = \frac{0.1}{s + 0.1} \quad (23)$$

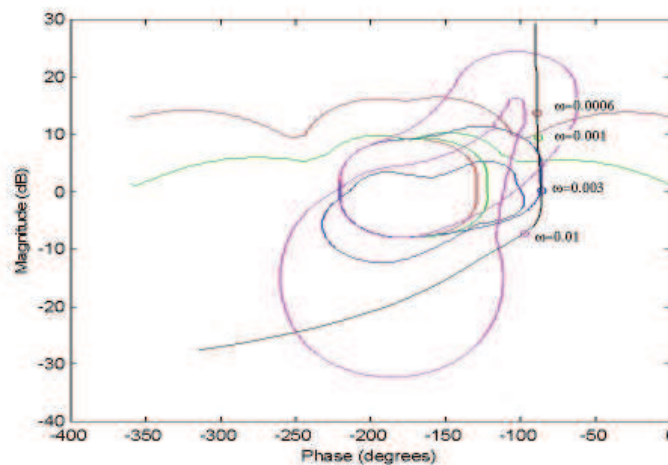


Fig. 25. Tracking and stability boundaries with the designed $L_0(j\omega)$

Figure 26 shows that the tracking specifications are fulfilled for all uncertain cases. Note that the different appearance of Bode diagrams in closed loop for five operating conditions is due to the changing root locus of $L(s)$ when the PID is introduced.

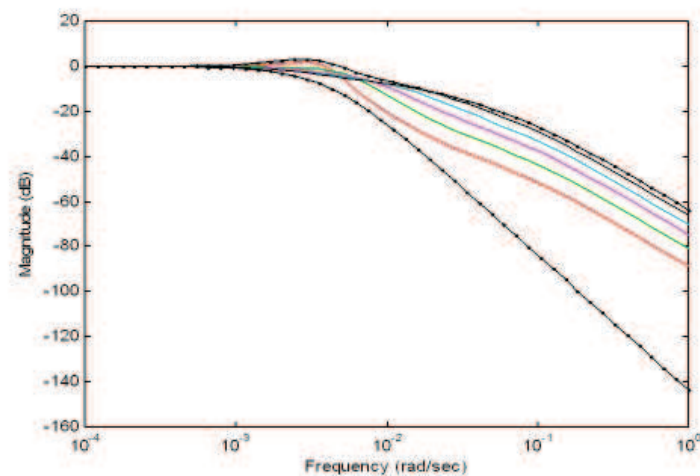


Fig. 26. Tracking specifications (dashed-dotted) and magnitude Bode diagram of some closed loop transfer functions

In order to prove the fulfillment of the tracking and stability specifications of the control structure, experiments were performed under several operating points and under different conditions of disturbances (Cirre et al., 2010), although only representative results are shown in this work.

Figure 27 shows an experiment with the robust controller. At the beginning of the experiment, the flow is saturated until the outlet temperature is higher than the inlet one (the normal

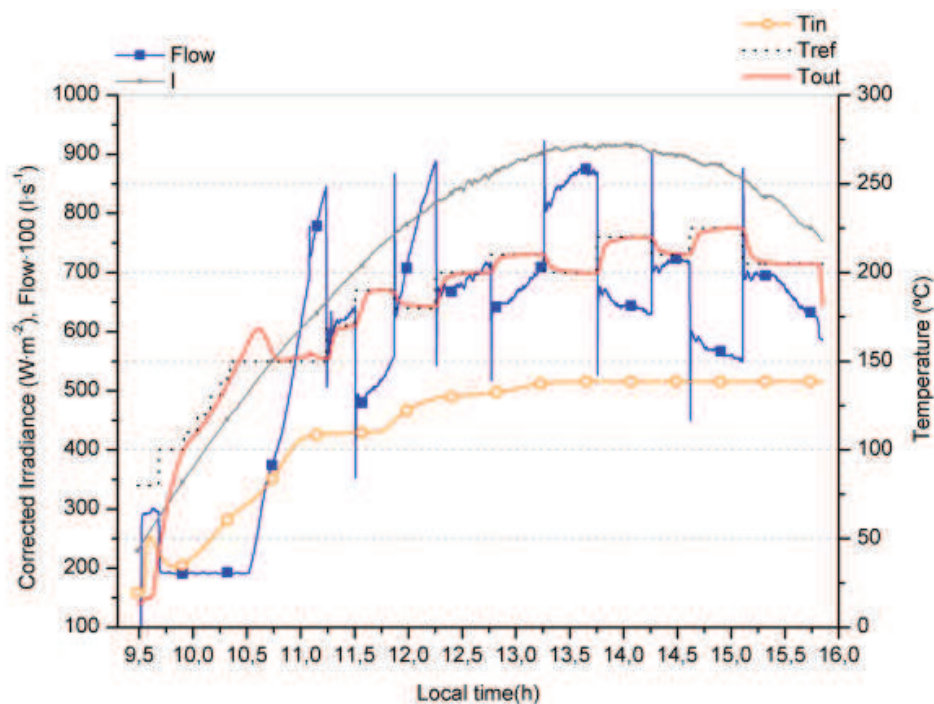


Fig. 27. QTF control results for the ACUREX plant (24/03/2009) (Cirre et al., 2010)

situation during the operation). This situation always appears due to the oil resident inside the pipes is cooler than the oil from the tank. Once the oil is mixed in the pipes, the outlet

temperature reaches a higher temperature than the inlet one. During the start up, steps in the reference temperature are made until reaching the nominal operating point. The overshoot at the end of this phase is 18 °C approximately, and thus the specifications are fulfilled. Analyzing the time responses, a settling time between 11 and 15 minutes is observed at the different operating points. Therefore, both time specifications, overshoot and settling time are properly fulfilled. Disturbances in the inlet temperature (from the beginning until $t = 12.0$ h), due to the temperature variation of the stratified oil inside the tank, are observed during this experiment and correctly rejected by the feedforward action (Cirre et al., 2010).

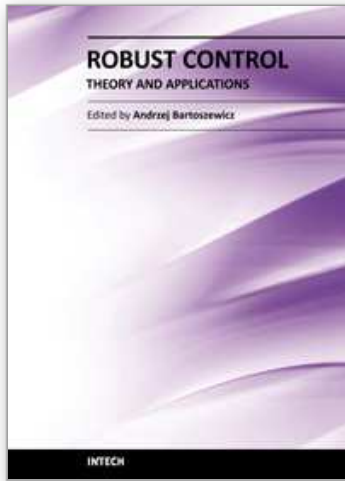
5. Conclusions

This chapter has introduced the Quantitative Feedback Theory as a robust control technique based on the frequency domain. QFT is a powerful tool which allows to design robust controllers considering the plant uncertainty, disturbances, noise and the desired specifications. It is very versatile tool and has been used in multiple control problems including linear (Horowitz, 1963), non-linear (Moreno et al., 2010), (Moreno et al., 2003), (Moreno, 2003), MIMO (Horowitz, 1979) and non-minimum phase (Horowitz and Sidi, 1978). After describing the theoretical aspects, the most well-known software tools to work with QFT have been described using simple examples. Then, results from two experimental applications were presented, where QFT were successfully used to compensate for the uncertainties in the processes.

6. References

- J.D. Álvarez, L. Yebra, and M. Berenguel. Repetitive control of tubular heat exchangers. *Journal of Process Control*, 17:689–701, 2007.
- M. Berenguel, E.F. Camacho, and F.R. Rubio. Simulation software package for the acurex field. Technical report, Dep. Ingeniería de Sistemas y Automática, University of Seville (Spain), 1994. www.esi2.us.es/rubio/libro2.html.
- C. Borghesani, Y. Chait, and O. Yaniv. *The QFT Frequency Domain Control Design Toolbox*. Terasoft, Inc., <http://www.terasoft.com/qft/QFTManual.pdf>, 2003.
- E.F. Camacho, M. Berenguel, and F.R. Rubio. *Advanced Control of Solar Plants (1st edn)*. Springer, London, 1997.
- E.F. Camacho, F.R. Rubio, M. Berenguel, and L. Valenzuela. A survey on control schemes for distributed solar collector fields. part i: modeling and basic control approaches. *Solar Energy*, 81:1240–1251, 2007a.
- E.F. Camacho, F.R. Rubio, M. Berenguel, and L. Valenzuela. A survey on control schemes for distributed solar collector fields. part ii: advances control approaches. *Solar Energy*, 81:1252–1272, 2007b.
- M.C. Cirre, J.C. Moreno, M. Berenguel, and J.L. Guzmán. Robust control of solar plants with distributed collectors. In *IFAC International Symposium on Dynamics and Control of Process Systems, DYCOPS*, Leuven, Belgium, 2010.
- J. M. Díaz, S. Dormido, and J. Aranda. Interactive computer-aided control design using quantitative feedback theory: The problem of vertical movement stabilization on a high-speed ferry. *International Journal of Control*, 78:813–825, 2005a.
- J. M. Díaz, S. Dormido, and J. Aranda. *SISO-QFTIT. An interactive software tool for the design of robust controllers using the QFT methodology*. UNED, <http://ctb.dia.uned.es/asig/qftit/>, 2005b.

- J.L. Guzmán, Rodríguez F., Sánchez-Hermosilla J., and M. Berenguel. Robust pressure control in a mobile robot for spraying tasks. *Transactions of the ASABE*, 51(2):715–727, 2008.
- I. Horowitz. *Synthesis of Feedback Systems*. Academic Press, New York, 1963.
- I. Horowitz. Quantitative feedback theory. *IEEE Proc.*, 129 (D-6):215–226, 1982.
- I. Horowitz and M. Sidi. Synthesis of feedback systems with large plant ignorance for prescribed time-domain tolerances. *International Journal of Control*, 16 (2):287–309, 1972.
- I. M. Horowitz. *Quantitative Feedback Design Theory (QFT)*. QFT Publications, Boulder, Colorado, 1993.
- I.M. Horowitz. Quantitative synthesis of uncertain multiple input-output feedback systems. *International Journal of Control*, 30:81–106, 1979.
- I.M. Horowitz and M. Sidi. Optimum synthesis of non-minimum phase systems with plant uncertainty. *International Journal of Control*, 27(3):361–386, 1978.
- K. R. Krishnan and A. Cruickshanks. Frequency domain design of feedback systems for specified insensitivity of time-domain response to parameter variations. *International Journal of Control*, 25 (4):609–620, 1977.
- M. Morari and E. Zafiriou. *Robust Process Control*. Prentice Hall, 1989.
- J. C. Moreno. *Robust control techniques for systems with input constraints, (in Spanish, Control Robusto de Sistemas con Restricciones a la Entrada)*. PhD thesis, University of Murcia, Spain (Universidad de Murcia, España), 2003.
- J. C. Moreno, A. Baños, and M. Berenguel. A synthesis theory for uncertain linear systems with saturation. In *Proceedings of the 4th IFAC Symposium on Robust Control Design*, Milan, Italy, 2003.
- J. C. Moreno, A. Baños, and M. Berenguel. Improvements on the computation of boundaries in qft. *International Journal of Robust and Nonlinear Control*, 16(12):575–597, May 2006.
- J. C. Moreno, A. Baños, and M. Berenguel. A qft framework for anti-windup control systems design. *Journal of Dynamic Systems, Measurement and Control*, 132(021012):15 pages, 2010.
- Y. Piguet. *Sysquake 3 User Manual*. Calerga Sàrl, Lausanne, Switzerland, 2004.
- C. J. Pritchard and B. Wigdorowitz. Mapping frequency response bounds to the time domain. *International Journal of Control*, 64 (2):335–343, 1996.
- C. J. Pritchard and B. Wigdorowitz. Improved method of determining time-domain transient performance bounds from frequency response uncertainty regions. *International Journal of Control*, 66 (2):311–327, 1997.
- L. Roca, M. Berenguel, L.J. Yebra, and D. Alarcón. Solar field control for desalination plants. *Solar Energy*, 82:772–786, 2008.
- A. Sánchez-Gimeno, Sánchez-Hermosilla J., Rodríguez F., M. Berenguel, and J.L. Guzmán. Self-propelled vehicle for agricultural tasks in greenhouses. In *World Congress - Agricultural Engineering for a better world*, Bonn, Germany, 2006.
- J. Sánchez-Hermosilla, Rodríguez F., González R., J.L. Guzmán, and M. Berenguel. A mechatronic description of an autonomous mobile robot for agricultural tasks in greenhouses. In Alejandra Barrera, editor, *Mobile Robots Navigation*, pages 583–608. In-Tech, 2010. ISBN 978-953-307-076-6.
- O. Yaniv, *Quantitative Feedback Design of Linear and Nonlinear Control Systems*. Kluwer Academic Publishers, 1999.



Robust Control, Theory and Applications

Edited by Prof. Andrzej Bartoszewicz

ISBN 978-953-307-229-6

Hard cover, 678 pages

Publisher InTech

Published online 11, April, 2011

Published in print edition April, 2011

The main objective of this monograph is to present a broad range of well worked out, recent theoretical and application studies in the field of robust control system analysis and design. The contributions presented here include but are not limited to robust PID, H-infinity, sliding mode, fault tolerant, fuzzy and QFT based control systems. They advance the current progress in the field, and motivate and encourage new ideas and solutions in the robust control area.

How to reference

In order to correctly reference this scholarly work, feel free to copy and paste the following:

José Luis Guzmán, José Carlos Moreno, Manuel Berenguel, Francisco Rodríguez and Julián Sánchez-Hermosilla (2011). A Frequency Domain Quantitative Technique for Robust Control System Design, Robust Control, Theory and Applications, Prof. Andrzej Bartoszewicz (Ed.), ISBN: 978-953-307-229-6, InTech, Available from: <http://www.intechopen.com/books/robust-control-theory-and-applications/a-frequency-domain-quantitative-technique-for-robust-control-system-design>

INTECH
open science | open minds

InTech Europe

University Campus STeP Ri
Slavka Krautzeka 83/A
51000 Rijeka, Croatia
Phone: +385 (51) 770 447
Fax: +385 (51) 686 166
www.intechopen.com

InTech China

Unit 405, Office Block, Hotel Equatorial Shanghai
No.65, Yan An Road (West), Shanghai, 200040, China
中国上海市延安西路65号上海国际贵都大饭店办公楼405单元
Phone: +86-21-62489820
Fax: +86-21-62489821

© 2011 The Author(s). Licensee IntechOpen. This chapter is distributed under the terms of the [Creative Commons Attribution-NonCommercial-ShareAlike-3.0 License](#), which permits use, distribution and reproduction for non-commercial purposes, provided the original is properly cited and derivative works building on this content are distributed under the same license.

IntechOpen

IntechOpen